MICHIGAN STATE UNIVERSITY

CYCLOTRON LABORATORY

THE QUARK-HADRON TRANSITION IN HEAVY ION PHYSICS AND THE EARLY UNIVERSE

DAVID H. BOAL

Lectures delivered at Michigan State University,
January, 1982

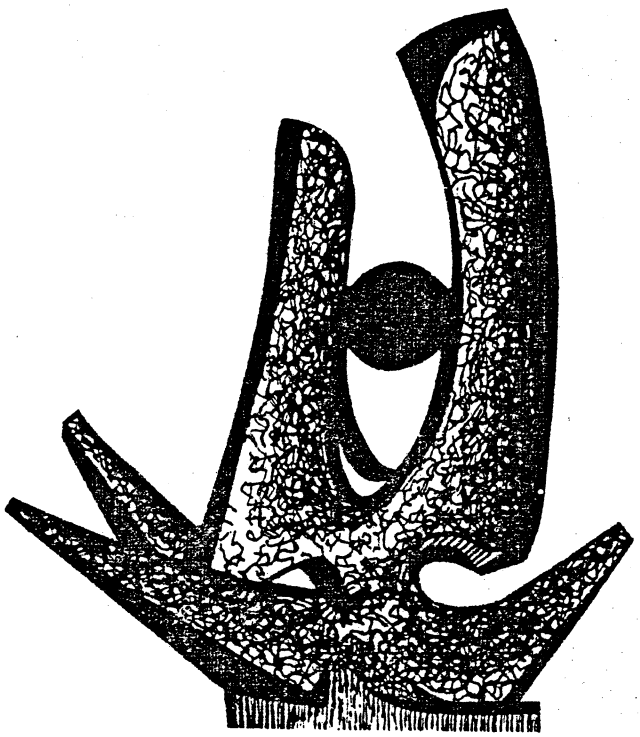

JUNE 1983

MSUCL-419

MSUCL-419
June 1983

THE QUARK-HADRON TRANSITION IN HEAVY ION PHYSICS AND THE EARLY UNIVERSE

David H. Boal

Lectures delivered at Michigan State University,
January, 1982

C O N T E N T S

Abstract

Several different models for the transition between hadronic matter and a quark-gluon plasma phase are reviewed. Each of the models involves different assumptions, and none can be said to be complete. However, they all generally predict the same range of temperatures (200-300 MeV at zero baryon number density) and baryon number densities (5-20 times nuclear matter density at zero temperature) for the phase transition to occur. A discussion of a likely means of accessing the transition in the laboratory, namely the central collision of relativistic heavy nuclei, is given. Both the accelerator energies required to attain the transition, and some of its experimental signatures, are presented. This transition may also have cosmological significance, both in the early universe and in the cores of dense stars. Only the former is discussed here: a review of the role of some nuclear and particle physics phenomena in the hot Big Bang model is given, and the effects of the relaxation of the confinement restriction on the condensation of quarks into hadrons is investigated.

1. INTRODUCTION

Our understanding of the nature of the constituents of hadrons has improved significantly in the two decades since the quark model was proposed.[1,2] Initially, quarks were regarded by some primarily as a bookkeeping tool, simply another mnemonic for keeping track of baryon or meson quantum numbers. Adding spin to the quarks allowed one to calculate normalized magnetic moments among other things,[3,4] and seemed to imply that the quarks had some dynamical significance. This conclusion was strengthened by the quark-parton model[5] which was used to explain aspects of high energy reactions involving hadrons. Further, it became apparent with the discovery of the ψ family of mesons[6-7] that one could treat quarks with the same methods as one used for atomic constituents, namely to construct a model for the potential energy of a quark-antiquark pair and solve for the energy levels of the bound pair. This approach[8] was refined considerably in the following years and evaluation of both the eigenvalues and eigenvectors (as measured in decay rates), for model potentials has been made for both mesons with heavy quarks[9] and baryons.[10] Of course, these calculations are sensitive to the form of the potential only over a limited distance range, say 1/10 to 1 fm. However, even starting with different parametrizations of the interquark potential, the same form seems to emerge once the parameters are made to reproduce, for example, bound state spectra. This behavior[11] is shown in Fig. 1.

Beyond this range of distances, where the concept of a potential may be less well defined, one has experimental evidence for the following characteristics. At short distances, the quarks must be weakly interacting in order to explain the scaling behavior of deep inelastic

scattering.[12-14] At large inter-quark separation, the interaction must become very strong, since free quarks have not yet been observed in accelerator experiments.[15] Whether quarks are permanently confined in hadrons is still a matter for both experimental[16-17] and theoretical[18-21] speculation.

Even if quarks are confined, in the sense that one cannot obtain a free quark in the absence of nearby hadronic matter, nevertheless one may be able to observe freely propagating quarks under special conditions. The situation may be like a conductor wherein electrons are free to travel within the conductor, but are not observed in isolation outside it. This possibility, that at certain densities and temperatures matter exists in such a form as to allow the free propagation of quarks in the hadronic medium either like a color conductor or like a quark plasma, will be the subject of this paper.

In the following section of this paper, several models of the quark-hadron transition will be presented. First, two simple arguments based on hadron close packing and percolation theory will be given. Then an overview of two approaches with more rigorous physics will be given: perturbative quantum chromodynamics and gluons on the lattice. Finally, calculations with explicit critical behavior, but less well defined physics will complete the section.

There are two areas of current application of this phenomenon: heavy ion physics and cosmology. Section 3 will contain a discussion of both the kinds of experimental conditions necessary to reach the transition region in relativistic heavy ion collisions, and possible signatures of the transition. The cosmological implications will be discussed in

Section 4. This section contains a review of the Big Bang model and some of the theoretical machinery used therein. This is followed by a discussion of the hadronic phases through which the early universe passed, and the observable consequences, if any, of each transition. Lastly, the effects of relaxing the quark confinement hypothesis are shown: the possibility of relic quarks left over from the condensation of the quark plasma into hadrons. Our conclusions will be summarized in the final section.

2. MODELS OF THE QUARK-HADRON TRANSITION

2.1 *Naive Expectations*

Central to the quark-hadron transition is the idea that as the density is increased, either through creation of hadrons by raising the temperature by hundreds of MeV or through compression of nuclear matter, perhaps in the core of a neutron star, or via both mechanisms, as one might expect in a heavy ion collision, the quarks in hadronic matter become more mobile. This probably results from two effects: first, the hadrons begin to significantly overlap, so it is difficult to say which quark belongs to which hadron, and second, the coupling between quarks becomes weaker at smaller interquark separation.

First, we will consider low temperatures and dense matter. As emphasized by Baym,[22] two distinct phenomena may occur as the hadron density increases. The first is that at some point nucleons become sufficiently dense that they become infinitely connected. At this density, the quarks are still localized in hadrons, but the hadrons, randomly distributed in space, form a "conducting" network such that a quark could, in principle, hop from one hadron to the next across the nucleus. This

kind of problem has been investigated numerically in percolation theory,[23-24] in which conducting spheres, for example, are placed on a lattice and the fraction of space, ρ_c, occupied by the volumes of the conducting spheres at which the system is infinitely connected, is calculated. The quantity ρ_c does not seem to be a strong function of the lattice type assumed, even though the fraction of sites occupied by the conducting spheres is. For the fcc, hcp and diamond lattice, ρ_c is[23] about 0.15 in 3 dimensions. Allowing the spheres to be randomly assigned to any point in space (with overlapping allowed) ρ_c changes to 0.29, the fraction of space occupied by the sum of the volumes being 0.34. Baym[22] chooses this latter value to estimate the density at which hadronic matter percolates. Assuming that the quarks are confined to a sphere of radius $r_0 = 0.8$ fm, then the critical density is $0.34/(4/3\ \pi r_0^3) \simeq 0.16$ hadrons/fm^3. This number is slightly less than that of normal nuclear matter ($n_0 = 0.17$ fm^{-3}), indicating that nuclear matter may already be percolated. Of course, if the quarks are confined to a very small sphere this number can easily be made larger than n_0.

The second transition Baym discusses is the more conventional one in which a uniform quark plasma, or liquid, is produced. This may be estimated in a simple minded way by using the density of spheres at close packing,[25] as illustrated in Fig. 2. The densities for cubic lattices are given in Table 1. For both cubic and hexagonal close packing, the fraction of volume occupied by touching hard spheres is 0.74. This is larger than that found for a simple cubic (0.52) or body centered cubic (0.68) lattice and about double ρ_c used to calculate the percolation density. With $r_0 = 0.8$ fm, one then finds the transition number density

is about 2 n_o. Since the hard core of a nucleon is typically quoted as about 0.5 fm, an upper bound for this density may be around 8 n_o. In any case, this simple argument gives a quark-hadron transition at T = 0 of several times nuclear matter density. We will return to more detailed estimates of this number below.

The other extreme condition at which simple estimates can be made is at zero net baryon number ($\Delta n_B = 0$) and high temperature. The summed hadronic number density for an ideal gas of hadrons as a function of temperature is plotted in Fig. 3. One can see that at temperatures above 200 MeV, the hadronic density is larger than either nuclear density or the reciprocal pion volume. The latter is probably the more relevant quantity since pions are the most copious hadron at these temperatures. This is illustrated for non-interacting hadrons at $\Delta n_B = 0$ in Fig. 4. Using a radius of 0.6 fm, more typical of a meson, the hexagonal close packing argument advanced above gives a transition density of 0.8 fm^{-3}, which corresponds to a temperature (from Fig. 3) of 180 MeV. A smaller radius would give a higher temperature.

We will not pursue further the thermodynamics of hard and soft sphere models here; the interested reader is referred to the literature.[26] What we have learned from these naïve geometrical arguments is that the hadron phase is bounded by a temperature of 200-300 MeV at zero baryon number density, and a net baryon number density of 2-8 n_o at zero temperature. These estimates are really only appropriate at the factor of 2 level, but nevertheless give the general range of T and Δn_B which are of interest. Before moving on to more sophisticated models, however, it is worthwhile checking what quark degrees of freedom are relevant at these temperatures.

From hadron spectroscopy and decay rates, it is now believed that there are at least five quark flavors and three colors of each flavor. The "at least" in the previous sentence reflects the fact that there are five quark flavors known from present spectroscopy, but a sixth is required for lepton-hadron equivalence (assuming that the τ lepton has a distinct neutrino). To obtain a crude estimate of the quark masses, one can simply take the lowest mass $J^P = 1^-$ particles (ρ, ϕ, ψ and Υ) and divide their mass by 2, since the quark content of these particles is predominantly a pair of identical quarks. This results in the quark masses shown in Table 2. It should be stressed that these masses are probably upper bounds, since they include the gluon contribution to the mass. This is particularly important for the u and d quarks, whose masses, after the confinement effects have been removed, are probably less than a tenth the value quoted here (see next subsection). Nevertheless, it is immediately obvious that the c,b and any heavier quarks will not have a significant role to play in the quark-hadron transition. For example, shown in Fig. 5 is the calculated number density for an ideal gas of charmed quarks of mass $m_c = 1.5$ GeV. Clearly, at a temperature of 300 MeV the number density is many orders of magnitude less than the massless quark limit. Hence, all of the calculations hereafter will include only u,d and s quarks.

2.2 *Quantum Chromodynamics*

The naïve models which we looked at in the previous section contained very little dynamics and were mainly geometrical. We will now turn to an approach which has far more physics, namely perturbative quantum chromodynamics.

The Feynman rules[27] for QCD are shown in Fig. 6. There is only one coupling constant, defined here as the bare coupling g, which appears in these diagrams. These diagrams are, of course, very similar to what one finds in QED with one major exception: QCD is a non-abelian gauge theory in which the gluons carry color "charge" and hence can couple to themselves; the photons in QED do not self couple. The difference in the couplings of the gauge particles in QCD and QED leads to different short distance behaviour.

First, a heuristic argument.[28] Suppose we define a bare charge in QED as e_0. At short distances, a photon probing this charge will measure e_0 itself. However, at larger distances, the polarization of the vacuum shields the charge, as shown in Fig. 7(a) and the effective charge seen by the photon probe is diminished. Hence, the effective charge increases at short distances in QED.

In QCD, the vacuum polarization shields the color charge [denoted by R in Fig. 7(b)] in the same way. However, because the gluons can self couple, then a virtual gluon emitted by a quark can be seen by the gluon probe [Fig. 7(c)]. This allows the quark to spread out its color charge in space: "anti-screening". This second effect turns out to be the dominant one, and therefore the effective charge decreases as short distances in QCD.

This effect is calculable, as can be seen from the following considerations. The bare quark-gluon vertex is shown in Fig. 8(a). However, this vertex in itself is not useful for calculating, for example, quark-quark scattering because of graphs such as those in Fig. 8(b), which will contain infinities. It can be shown[29] that the sum of these

graphs can be replaced by the single graph in Fig. 8(a) with g no longer being constant, but rather being a function of the four-momentum transfer squared, $-Q^2$, at the vertex. The strong interaction analogue of the electromagnetic fine structure constant

$$\alpha_s = g^2/4\pi \tag{1}$$

is given as a function of Q^2 through

$$\frac{4\pi}{\alpha_s(Q^2)} = \frac{4\pi}{\alpha_s(\mu^2)} + \left(11 - \frac{2}{3} n_f\right) \log \frac{Q^2}{\mu^2} + O(\log \log Q^2) . \tag{2}$$

The $\log Q^2$ term arises from order α corrections, and the $\log \log Q^2$ terms from order α_s^2. The coupling constant must be fixed at some value of Q^2, chosen here as μ^2, just as in QED. The quantity n_f is the relevant number of quark flavors at Q^2. The log log terms are often dropped from Eq. (2), so that it can be rewritten as

$$\alpha_s(Q^2) = \frac{4\pi}{\left(11 - \frac{2}{3} n_f\right) \log\left(\frac{Q^2}{\Lambda^2}\right)} \tag{3}$$

where Λ is a parameter to be determined by fixing α_s at some Q^2. While there are many different ways of fixing Λ, the range of values obtained is usually 100-500 MeV. Shown in Fig. 9 is the behavior of $\tilde{\alpha}_s(Q^2) \equiv \alpha_s(Q^2)/4$. (We choose $\tilde{\alpha}_s$ to facilitate comparison with the calculation to follow.) One can see that this function has the behavior which was hinted at above: it is large at small Q^2 (long distance) and small at large Q^2 (short distance). It should be pointed out that the form given by Eq. (3) has an unphysical pole at $\sqrt{Q^2} = \Lambda$. This arises from the neglect of higher order (in α_s) terms in writing Eq. (3). The pole can be moved to a physical location ($-Q^2$ timelike) through a prescription such as[30]

$$\alpha_s'(Q^2) = \frac{4\pi}{\left(11 - \frac{2}{3} n_f\right) \log\left(1 + \frac{Q^2}{\Lambda^2}\right)} \quad . \tag{4}$$

This form has the property that it gives rise to a linear potential ($V \sim ar$) for the quark-quark potential at small Q^2. The form of $\tilde{\alpha}_s' = \alpha_s'/4$ is also shown on Fig. 9 for Λ = 500 MeV.

The masses of the quarks also become a function of Q^2, and can be calculated using renormalization group techniques. One finds[31]

$$\frac{M}{m_f} \frac{dm_f}{dM} = \gamma_f(g, m_f/M) \tag{5}$$

where, to lowest order in g the functions γ are given by the approximate expression:

$$\gamma_f \approx \frac{-g^2}{2\pi^2} \frac{1}{1 + 2m_f{}^2/M^2} \tag{6}$$

where $M \equiv \sqrt{Q^2}$ and m_f is the mass of the quark with flavor f. It is clear from the minus sign in γ_f that as M increases, m_f decreases, leading to asymptotically massless quarks at large M. The behavior of the u-quark mass as a function of temperature found in the calculation described below is given in Fig. 10 [for α given by Eq. (3)]. This kind of behavior, that the quark mass becomes singular in some temperature and density regions, is related to the confinement idea that a quark cannot go on mass shell.[32]

To make use of these results in the problem at hand, one needs a way of relating Q^2 with the temperature of the system. An approach suggested by Kapusta,[33] is to use

$$Q^2 = \frac{4}{3} \frac{\sum_i n_i \langle \vec{k}^2 \rangle_i}{\sum_i n_i} \tag{7}$$

where there is a sum over the i species present, each with a number

density n_i. The quantity $<\vec{k}^2>_i$ is the thermal average of the three-momentum of species i. For example, in a system comprising of only massless quarks and no gluons,

$$n_i = \frac{3}{4}\frac{\zeta(3)}{\pi^2} T^3 \tag{8}$$

and

$$<\vec{k}^2>_i = \frac{1}{n_i}\frac{45}{4}\frac{\zeta(5)}{\pi^2} T^5 \tag{9}$$

where $\zeta(r)$ is the Riemann Zeta function $\left(\text{equal to } \sum_{n=1}^{\infty} (1/n)^r\right)$, so that $\sqrt{Q^2} \approx 4T$. On this basis one can see from the behavior of $\tilde{\alpha}_s$ in Fig. 9 that for temperatures in the 200 MeV region or less (depending on which form one chooses for α_s) the coupling is going to become strong and we can expect the quarks to bind into hadrons.

To put all of these ingredients into a QCD generated equation of state and find a quark-hadron phase transition has not been done. Rather, the QCD motivated attacks on this problem have followed 3 lines:

i) perturbative QCD expansions of the pressure in terms of α_s, with neglect of non-perturbative effects

ii) investigation of the role of semiclassical, non-perturbative solutions (instantons) in QCD

iii) lattice gauge theory calculations.

We will deal with each of these approaches in turn.

It has now been about a decade since finite temperature and density effects in gauge theories began to be investigated vigorously.[34-40] The approach taken in perturbative QCD calculations at finite temperature has been to expand the pressure in a power series in α_s:

$$P = P_0 + P_2 + P_3 + \ldots \tag{10}$$

where the subscripts refer to the power of g involved. Perturbative QCD

calculations have been done by a number of authors[41-44] with the series truncated at P_4 for massless quarks and P_3 for massive ones. There is some question[39] as to how far this perturbation series can be carried; in particular, P_6 and higher terms may be incalculable. For our purposes, we shall simply quote a few of the results of the massive quark calculation[33] at zero net baryon number density, the reader being referred to the literature for details.

The ideal gas contribution to the pressure is given by

$$P_o = \frac{4}{3} N_c \sum_f \int \frac{d^3p}{(2\pi)^3} \frac{\vec{p}^2}{E_p} \eta_p + \frac{\pi^2}{45} N_g T^4 \tag{11}$$

where there is a sum over quark flavors, f, and there are N_c colors of quarks and, correspondingly, $N_g = N_c^2 - 1$ gluons. Here,

$$\eta_p = [\exp(E_p/T) + 1]^{-1} \tag{12}$$

which is different from the definition used in Ref. 33. The second order term is a sum of two pieces,[33]

$$P_2 = P_2^{exch} + P_2^{gluon} \tag{13}$$

with

$$P_2^{gluon} = -\frac{1}{9} \tilde{\alpha}_s \pi N_c N_g T^4 \tag{14}$$

and, for $\Delta n_B = 0$:

$$P_2^{exch} = -\frac{8}{3} \pi \tilde{\alpha}_s N_g T^2 \sum_f \int \frac{d^3p}{(2\pi)^3} \frac{\eta_p}{E_p} - 8\pi \tilde{\alpha}_s N_g \sum_f \int \frac{d^3p}{(2\pi)^3} \frac{d^3q}{(2\pi)^3}$$

$$\times \frac{\eta_p \eta_q}{E_p E_q} \left\{ \left[\frac{2m^2}{(E_p - E_q)^2 - \omega^2} + 1 \right] + \left[\frac{2m^2}{(E_p + E_q)^2 - \omega^2} + 1 \right] \right\} . \tag{15}$$

The quantity ω is defined by

$$\omega = |\vec{p} - \vec{q}| \tag{16}$$

Lastly, the plasmon term is given by

$$P_3 = \frac{8}{3\pi^2\sqrt{2\pi}}\,\tilde{\alpha}_s^{3/2}\,N_g\,T\left[\frac{2}{3}\pi^2 N_c T^2 + 2\sum_f \int_0^\infty \frac{dp}{E_p}(p^2+E_p^2)\eta_p\right]^{3/2}. \quad (17)$$

To perform the numerical work,[33] a value of the scale parameter Λ is chosen (500 MeV) and the quark masses are assigned ($m_u:m_d:m_s$ = 1 : 1.8 : 36 at large M, m_s = 300 MeV at M = 1 GeV). The equations for the pressure are then solved iteratively since the expressions for the coupling constant, masses and subtraction point (M) at any given T are coupled. The ratios of $-P_2/P_0$ and P_3/P_0 are plotted in Fig. 11.

One sees that, for temperatures of 1000 MeV and above, the second and third terms of the perturbative series are about 10% of the first term in magnitude. The series is not particularly convergent but P_2 and P_3 do have the opposite sign and hence the pressure (if the series is truncated at P_3) is close to the ideal value. P_3 does not become less than P_2 in magnitude until much higher temperatures than those considered here because the coupling constant depends only logarithmically on the temperature. The question of how large P_4 is compared to P_3 has not been answered for massive quarks, so it is difficult to say whether the series diverges badly.

At temperatures below 1000 MeV, the deviation of the pressure from ideality becomes much stronger, with $P_0 + P_2 + P_3$ becoming many times larger than the ideal value at $T \approx 200$ MeV, or even negative if only $P_0 + P_2$ are kept. Although a breakdown in perturbation theory is what one would expect as one neared the transition point, it is difficult to assign a meaningful temperature to the quark-hadron transition in this approach precisely because of the poor behavior of the series. Because of the lack of a physically sound procedure for estimating the transition

temperature (see the discussion in Ref. 45 for example), this calculation really only tells us that the transition should occur in the hundreds of MeV range for $\Delta n_B = 0$. This estimate is not strongly influenced by the unphysical pole in α_s as defined by Eq. (3). The P_3/P_0 ratio still passes through unity at $T \approx 600$ MeV even if Eq. (4) is used instead, since the values of α and α' are not much different at this temperature.

Kapusta[33] has investigated this model at finite Δn_B (i.e., non-zero chemical potential) as well, and found that the temperature at which the series diverges decreases with increasing Δn_B.

To get a more accurate measure of the transition temperature one must somehow include the non-perturbative effects not present in the above calculation. A discussion of the effects of instantons (which have been calculated by many authors)[45-49] is beyond the scope of these lectures, and the interested reader is referred to the reviews[45,46] of these calculations. The only point which we wish to make here is that the instanton pressure at high temperature does not shift the QCD calculation away from the ideal gas result. At low temperature, adding instantons to the QCD calculation simply indicates a higher temperature for the breakdown of perturbation theory. Calculations involving instantons alone have been performed and do show critical behavior.[49]

The last approach which we wish to mention in this section is that of lattice gauge theory. Although this theory has had difficulty incorporating fermions (so in QCD the calculations described here deal with gluons only) and does not possess a well understood continuum limit, nevertheless it can be calculated in the strong coupling regime. Again, it is not the purpose of these lectures to record these calculations in detail, so the

interested reader is referred to Refs. 50-54 and the references therein for the techniques involved.

One of the properties of the lattice calculations is that they are capable of producing a confining "potential" which grows linearly with the interquark separation r:

$$V = \sigma r \ . \tag{18}$$

Such a relationship between energy and distance was used in the massless string model wherein the energy per unit length of the string is a constant (the string constant, σ):

$$dE = \sigma d\ell \ . \tag{19}$$

The energy of such a string whose ends rotate at the speed of light is[55-56]

$$E^2 = 2\pi\sigma \ J \ . \tag{20}$$

where J is the angular momentum. This expression is familiar from the Regge trajectory analysis of differential cross sections, the universal Regge slope α being related to σ via

$$\alpha = (2\pi\sigma)^{-1} \ . \tag{21}$$

An average value of α would be[57] 0.95 GeV^{-2}, giving a value to σ of 0.17 GeV^2, which is what will be used in the calculations of this paper.

Both Monte Carlo methods and semiclassical methods using an effective action have been used to investigate a model with only gluons on a lattice. We will deal with the Monte Carlo calculations first, although both approaches give similar results.

It was found,[58-59] for an $SU(2)_c$ theory [i.e. SU(2) in color] that there were two distinct coupling regimes at zero temperature: σ being either large or small (discontinuously) depending on the bare coupling of the gluons. This suggested that the theory might change from a

strong coupling regime at low temperatures to a weak coupling at high temperature. This was in fact shown to be the case by several workers[60-62] in $SU(2)_c$ and, more recently,[63] $SU(3)_c$. For example, in $SU(2)_c$ it was shown that[62] the energy density of gluon matter had the expected T^4 dependence at high temperature, the specific heat showing a cusp (in a Monte Carlo sense) at around $T_c \approx (40 \pm 2)\Lambda_L$, where Λ_L is the lattice scale parameter. The quantity Λ_L is related to the zero temperature string constant σ_0 via[58]

$$\Lambda_L = (1.3 \pm 0.2) \times 10^{-2} \sqrt{\sigma_0} \ . \tag{22}$$

Using the value of σ_0 quoted above, this gives a transition temperature of about 210 MeV.

This same kind of behavior was observed in a semiclassical effective lagrangian approach used by Callan, Dashen and Gross.[64-65] The sharp strong to weak coupling transition observed at $T = 0$ disappears around $T_c = 30\text{-}40\ \Lambda_L$, in agreement with the Monte Carlo results.

2.3 *A Mean Field Calculation*

An approach to the quark-hadron transition which is less well founded in the particle physics sense but does possess a well defined transition point involves an extension of a method used by Olive[66] in explicit two-phase calculations (discussed in the next subsection). The calculation proceeds as follows:[67]

The number density per spin degree of freedom for non-interacting particles is given by

$$n_i = \frac{1}{(2\pi)^3} \int d^3q_i (\exp[E_i/T] \pm 1)^{-1} \tag{23}$$

where the +(-) sign refers to fermions (bosons). As before, units in

which $h = c = 1$ are used, and Boltzmann's constant has been absorbed in the temperature. The energy E is the relativistic

$$E = (m^2 + q^2)^{1/2} \quad . \tag{24}$$

This expression is for zero chemical potential, i.e. equal numbers of particles and antiparticles. To allow for unequal numbers of fermions and their antiparticles, Eq. (23) would read:

$$n_i = \frac{1}{(2\pi)^3} \int d^3q_i \, (\exp[E_i \mp \mu)/T] + 1)^{-1} \tag{25}$$

where the sign convention used here will be -(+) for fermions (anti-fermions) so that $\mu > 0$ corresponds to $\Delta n_B > 0$. Equation (23) has two simple limits for bosons:

$$T >> m \qquad n_i = \frac{1.202}{\pi^2} T^3 \tag{26}$$

$$T << m \qquad n_i = \left(\frac{mT}{2\pi}\right)^{3/2} \exp(-m/T) \quad . \tag{27}$$

For fermions, Eq. (26) must be multiplied by a factor of 3/4.

The mean field calculation[68] used here involves changing the energy in Eq. (24) by an amount V to account for the mean interaction of a particular quark or gluon with the background "sea" of particles. This can be done either through introducing an effective mass

$$E \to [(m_o + V)^2 + q^2]^{1/2} \tag{28}$$

or a background potential

$$E \to (m^2 + q^2)^{1/2} + V \quad . \tag{29}$$

We will follow the effective mass calculation here, and the reader is referred to Ref. 67 for details of the other approach.

It was mentioned above that in lattice gauge theories, the confining piece of the quark-quark potential, which we will define as V_{qq}, has a power law behavior of the form[50-54,69]

$$V_{qq} = \sigma r \tag{30}$$

where σ has a value of about 0.17 GeV^2 from the Regge trajectory analysis of high energy cross sections. To use this potential in a mean field sense, one must replace r in favor of a number density. The simple substitution

$$r = \left(\sum_i n_i\right)^{-1/3} \tag{31}$$

where the sum is over all hadronic species[70] is a first approximation (of Table 1) appropriate for our purposes here. Hence, the identification

$$V = \sigma\left(\sum_i n_i\right)^{-1/3} \tag{32}$$

will be made. This form of the potential has the kind of limiting behavior which is expected from QCD. At large T, the number densities will be large and hence V will be small. The number density equation (23) will then simply give the ideal gas result. At low temperatures, the number densities will be small and hence the quark-quark interaction will be large. This will lead, as we will show, to substantial deviations from ideality. Of course, the potential in Eq. (32) is a power law one and will not exactly mimic QCD, from which one might expect to see logarithmic terms. Nevertheless, the overall behavior will be similar.

If one substitutes this expression for V (or in fact, any expression which involves taking the number density to an inverse power) into Eq. (23) for either the background potential [Eq. (29)] or effective mass [Eq. (28)] approach, then one obtains an expression which can be solved for n as a function of T. However, the interesting property of this equation is illustrated graphically in Fig. 12 for $\mu = 0$ in the background potential

approach. Three flavors of massless quarks and eight gluons have been chosen as an example, and the rhs of Eq. (23) is plotted against n_i, the quark number density for a particular spin state. One observes that there are three solutions (including $n_i = 0$) to the equation at large T, the one with the larger n_i has the lower free energy and connects smoothly with the ideal gas expression as $T \to \infty$. However, as the temperature decreases, the two non-trivial solutions approach each other until they are identical at some T_c. Below this temperature, only the trivial $n_i = 0$ solution exists. Hence, one sees that this approach has the kind of behavior expected from QCD and lattice gauge theory: ideal gas at large T, deviations from ideality as the temperature decreases, disappearance of the quark-plasma phase below some transition temperature T_c. Although this critical behavior has been illustrated here for $\mu = 0$, it persists for $\mu \neq 0$ as well (although in a different form).

In general, because V depends on both quark and gluon number densities, one actually has to solve a group of coupled equations like Eq. (23) for each particle species. There are, however, two conditions under which an approximate expression can be obtained for the transition point, assuming massless particles.

One can define η as the effective number of spin degrees of freedom from

$$\eta = \left(\sum_i n_i \right) / n_{spin} \tag{33}$$

where n_{spin} will be defined as the ideal boson gas expression

$$n_{spin} \equiv \frac{1.202}{\pi^2} T^3 \ . \tag{34}$$

For example, for 3 flavors of quarks and 8 gluons, $\eta = 2 \times 8 + 3/4(3 \times 3 \times 2 \times 2)$

if there are equal numbers of quarks and antiquarks. Defining

$$\kappa \equiv \sigma\pi^{-1/3} , \tag{35}$$

the transition temperature at $\mu = 0$ is approximately

$$T_c \simeq \left[\kappa^2 \, 2\pi \left(\frac{2e}{9}\right)^3\right]^{1/4} \tag{36}$$

in the effective mass calculation. In the above example, this gives a temperature of 240 MeV. Similarly, at zero temperature, the critical chemical potential in the effective mass calculation is

$$\mu_c = (2\kappa(6\pi^2)^{1/3})^{1/2} \tag{37}$$

giving rise to a quark density per spin degree of freedom of

$$n_{ic} = (\kappa^3/6\pi^2)^{1/2} . \tag{38}$$

The gluon and antiquark number densities are both zero at $T = 0$. The net baryon number density at $T = 0$ for two flavors of massless quarks is simply four times n_{ic}, or 1.38 fm^{-3} for σ = 0.17 GeV^2. Similar expressions can be obtained for the background potential model; in fact the expression for n_{ic} is identically the same, although μ_c is larger by $\sqrt{2}$. These estimates for the transition, T = 240 MeV at $\Delta n_B = 0$ and $\Delta n_B \approx 8\, n_o$ at $T = 0$, are similar to what was obtained from the naïve models of Section 2.1.

For intermediate values of T and Δn_B, one must go to the computer and find the point at which the solution to the coupled quark and gluon density equations vanishes. The result of such a calculation for both the effective mass and background potential models is shown in Fig. 13. These calculations used 8.3, 15 and 300 MeV as the bare masses of the u, d and s quarks respectively. The "size" of the hadronic phase is proportional to the value of σ in V: From dimensional arguments alone, $T_c \propto \sigma^{1/2}$ and $n_{ic} \propto \sigma^{3/2}$. If σ is larger than the value assumed here,

then the hadronic domain will be larger *etc.*, and hence there is probably a 30% or so error on the estimated domain of the hadron phase.

Before leaving this section, it is worthwhile commenting on the quark mass. In the effective mass approach, the quark mass is a sum of the bare quark mass and V, the mean potential. Shown in Fig. 14 is the mass shift of the quark mass as a function of temperature in the effective mass calculation at $\mu = 0$. As with QCD, one observes that the quark mass increases as the temperature decreases, becoming infinitely large (in the sense that $V \to \infty$ as $n \to 0$) below the transition temperature. This is another reflection of confinement, that it takes infinite energy to put a quark on-mass-shell in the hadron domain.

2.4 *Other Models*

The calculations which have been presented in the previous subsections have had the common characteristic that they have used only a single theoretical framework to delineate the quark-hadron transition region. In QCD, one can in principle calculate both the bound state properties of hadrons and the high temperature behavior of the quark-gluon plasma with the same theory. The lattice gauge theory calculations similarly evaluate quantities such as the string tension or specific heat as a function of temperature for both the free and condensed phases. Lastly, the phenomenological mean field model presented in the last subsection uses one prescription for calculating the thermodynamic properties of the quark-plasma phase, and finds that the phase vanishes for a particular region of temperatures and baryon number densities.

A wholly different approach will be reviewed in this subsection.

These calculations involve developing separate models to describe the quark and hadron phases, and then comparing the free energies of the models as a function of temperature *etc.* Some of these calculations have been done only at $T = 0$ or $\Delta n_B = 0$, although a few of them allow one to calculate the entire phase diagram as in Fig. 13. Because one develops separate models for the two phases in these calculations then a phase transition is almost guaranteed: the thermodynamic properties must exhibit some discontinuity simply because the models are independent. While these models are not in general useful in predicting the nature of the phase transition (first order *etc.*), nevertheless they are valuable as confirmation of the ideas introduced above and can be used to define better the transition region and, possibly, its experimental signature.

The simplest two phase model which one could postulate is an ideal gas model in which the free energy of an ideal gas of quarks and gluons is compared with an ideal gas of hadrons. The ideal gas expression for the number density per spin state was given in Eq. (23), while the expressions for the energy density U and pressure P per spin state at zero chemical potential are:

$$U_i = \frac{1}{(2\pi)^3} \int E_i \, d^3q_i \, (\exp[E_i/T] \pm 1)^{-1} \tag{39}$$

and

$$P_i = \frac{1}{3} \frac{1}{(2\pi)^3} \int (q_i^2/E_i) \, d^3q_i \, (\exp[E_i/T] \pm 1)^{-1} \, . \tag{40}$$

The entropy is then obtained from

$$S = \frac{1}{T} (U + P) \, . \tag{41}$$

Both the entropy and the free energy (which is the negative of the pressure) of the two phases cross, as one might expect. Shown in Fig. 15 is

the result of a calculation of the pressure of the two phases (including leptons) for hadrons up to 1.5 GeV in mass. The cross-over point is in the 300-350 MeV temperature region. However, the phases are reversed to what one would expect: at low temperature the species with the greater pressure (lower free energy) are the massless gluons, and at high temperature it is the rapidly increasing number of hadronic species. It is crucial that the interactions among hadrons or quarks and gluons be taken into account to avoid this phase reversal and suppress the hadron and quark-gluon pressures in the appropriate region. It is clear that, because of the shallow intersection of the two free energy curves, the estimated transition temperature will be a sensitive function of the way in which the interactions are handled. Olive[66] has used a mean field calculation, like the one used above, for both of the phases. Although many assumptions must be made about the hadronic interactions, he is able to demonstrate that the phases do come out in the expected fashion, with a transition temperature of about 400 MeV at zero chemical potential. Karsch and Satz[71] use an excluded volume argument to produce deviations from ideality for a gas of mesons, and find a temperature of the order of the pion mass (140 MeV) for the transition, again at zero chemical potential.

Another approach[72] has been to use the MIT bag model[73-74] to describe the pressure of the quark phase, and a mean field theory[68,75] and other models to describe the nuclear matter phase, at zero temperature. Comparison of the free energies gives a transition density of 12-18 n_o, but the result is highly model dependent, ranging from 7 to 42 n_o. This approach has been extended[76] to include pions at finite

temperature, and gives a phase diagram similar to Fig. 13, although again the result is model dependent.

A variant on the above approach has been to use a nuclear matter model for the hadron phase, and a QCD calculation for the quark phase. Depending on the model, baryon number densities in the 10-20 n_o range are obtained.[77] A related calculation[78] shows critical behavior for temperatures less than 200 MeV. Lastly, a Hartree-Fock version of quark matter developed by Alvarez[79] yields $\Delta n_B \sim 30\ n_o$ at $T = 0$.

To summarize, the explicit two phase calculations show a similar range of T and Δn_B for the transition region as do the previous calculations. The temperatures at $\Delta n_B = 0$ are typically in the 200 MeV region, and the number densities at $T = 0$ are in the 10-20 n_o range, with some spread. Because the wide variety of techniques and approximations described above give a phase diagram whose average is not too removed from Fig. 13, we will conclude that there is indeed a quark-hadron phase transition, although a good calculation of its boundary is not yet available. Because the model of Section 2.3 does fall near the "average" of many other calculations, we will use it in the following sections in which the experimental and cosmological consequences of this phase transition will be investigated.

3. HOT, DENSE MATTER IN THE LABORATORY

3.1 *Relativistic Heavy Ion Collisions*

The calculations presented above are certainly far from the last word on the quark-hadron transition, in that none of these approaches represent a complete theory of strong interaction dynamics over the temperature range of interest. However, the calculations do point to a

phase transition occurring at energies and baryon densities which may be accessible in the laboratory. We now turn to the twin questions of under what conditions can one access this transition, and what would be its experimental signature. Satisfactory answers to these questions are more scarce than they were for the question of determining the quark-hadron phase diagram, but nevertheless progress is being made and some tentative conclusions can be drawn.

The most obvious place to seek the kinds of densities and temperatures appropriate for this transition is in the central collision of relativistic heavy nuclei. A model in which the participating nucleons in the collision undergo such a large number of internucleon interactions that they form a thermally equilibrated system (on the hadronic time scale) has achieved considerable success[80] in describing these reactions. The temperatures associated with these reactions, even at current accelerator energies, already are in excess of 100 MeV. It is easy to imagine boosting current accelerator energies to the point where temperatures in the 300 MeV region can be reached.

To estimate what range of laboratory energies would be required for such an accelerator, we first perform a very crude calculation and then discuss some caveats. The calculation has appeared in several guises in the literature,[33,76,81-83] and we will adopt the following version:

It will be assumed that in the central collision of two equal mass heavy ions, all of the nucleons and their kinetic energy are trapped in a volume equal to the Lorentz contracted volume of one of the heavy nuclei in the center of mass frame. The results of this calculation are shown as the solid curve in Fig. 16. The energy density, rather than

the temperature, has been plotted because in order to attain the plasma phase, a latent heat must be added, making the energy density a more relevant quantity.

The relationship between the energy density and the temperature at relativistic energies is the following. The relativistic energy density (for bosons) per spin degree of freedom is

$$u_i = \frac{\pi^2}{30} T^4 \qquad (43)$$

giving an energy per particle of 2.7 T. If this is equated to the center of mass energy per nucleon of the heavy ions, E_{cm}, then the lab energy per nucleon, E_{lab}, is related to T via the extreme relativistic expression

$$E_{lab} = \frac{2}{m_N} E_{cm}^2 = 15.5\ T^2\ (\text{GeV}) \ . \qquad (42)$$

Ignoring latent heats, a lab energy in the 10 GeV per nucleon range should suffice to attain the transition region.

Of course, the above calculation is a gross oversimplification of what may actually happen in a heavy ion collision. No attention has been paid to the detailed NN interaction and whether there is sufficient momentum transfer per collision to deposit a large fraction of the heavy ions' kinetic energy in the interaction region in a way that would lead to thermalization. Calculations performed with a cascade code[84] do confirm a temperature on the order of a hundred MeV and a baryon density of at least double nuclear density as being attainable for an incident lab energy of 2 GeV per nucleon. However, the temperature should not rise rapidly above this as the incident energy is raised. This is because the differential cross sections for the elementary NN interactions become strongly forward peaked as the incident energy is raised above a

few GeV, meaning that the nuclei have a greater chance of simply passing through one another. Increasing the incident energy from 2 to 20 GeV per nucleon may only raise the temperature by 50-100 MeV.

One can compare the energy densities obtained for heavy ion collisions in this simple model with the energy densities required for the transition by use of the model in Section 2.3. In evaluating the energy density, an extra term, f(n), must be added to the usual expression,

$$U = \frac{1}{(2\pi)^3} \sum_i \int E_i d^3q_i \left\{ \exp[(E_i \pm \mu)/T] \pm 1 \right\}^{-1} \qquad (44)$$

to account for possible double counting of the potential.

For the background potential calculation (see Refs. 66 and 67) this term is given by

$$f(n) = (\kappa/2) n_{TOT}^{2/3} . \qquad (45)$$

It was not possible to find an analytical expression for f(n) in the effective mass calculation, but it could be demonstrated that Eq. (45) is an upper bound in this case. The results of this calculation for the energy density are shown in Fig. 16. Arguing from the energy density point of view, the lab energy of the heavy ion collision required to access the phase transition is significantly higher, namely 20-25 GeV per nucleon, than what one gets from temperature arguments alone. The kind of laboratory energies are within the realm of current technology, and have already been achieved for α-α collisions at CERN. Hence, the quark-hadron transition should soon be within the experimentalists' grasp.

3.2 *Experimental Signatures of the Transition*

Now that we see that the transition region should be attainable with an accelerator capable of producing heavy nuclei with lab kinetic energies in the 30 GeV per nucleon range, we must ask how will we recognize the phase transition when we see it. As was said previously this question is much more difficult to answer than the previous ones.

Let's pause for a moment and look at what we would expect to see if there were no quark plasma. Shown in Fig. 17 is a qualitative estimate of what the distribution of temperatures might look like in a nuclear fireball at a few $\times 10^{-23}$ seconds after thermal equilibrium has been reached. The hot core is expanding and cooling, and is surrounded by a cool gas of hadrons. One would expect[85] that particles with a long mean free path in nuclear matter, such as K^+ mesons, could escape from the core and carry information about its temperature. Particles with short mean free paths, such as π mesons, would interact repeated on their way out of the core and would carry information about the surface temperature. This scenario is consistent with what is observed experimentally. If one uses the exponential slopes of the inclusive differential cross sections as a measure of the temperature of the source which emitted the particle, then it is observed that $T_{K^+} > T_p > T_\pi$.

If there is a quark plasma in the core of a nuclear fireball, then the situation might be as illustrated in Fig. 18. One would expect the same ordering of temperatures as before, for K^+, and π probes, for example, only this time the hadrons most likely will originate from the plasma's surface boundary. Hence, the hadronic ejectiles will probably simply be a measure of the surface temperature of the plasma. For

baryon densities in the few times nuclear density regime, this surface temperature is likely to be in the 150-200 MeV range, to judge by Fig. 13. As a function of bombarding energy, then, what one would expect to see is the temperature (measured hadronically) rising from some small value at low bombarding energies, up to a value of 150 to 200 MeV at a lab energy of 10-20 GeV per nucleon, and then remain roughly constant at higher bombarding energies.

There is a hint that this behavior might be emerging from various high energy experiments. Shown[86-87] in Fig. 19 is the estimated temperature as a function of bombarding energy obtained from various projectiles. Because heavy ion data is not available at the high energies required to investigate the transition region, one must piece together various projectiles and hope that they have a common mechanism. This may be a very strong assumption and prove to be false. One sees that the behavior of the fireball temperature is consistent with the ideas outlined above.

Of course, this experimental result even if shown to be valid in high energy heavy ion reactions may be attributable to some other phenomenon entirely. For example:

1. The maximum temperature attainable may rise only slowly with incident energy, as alluded to in Section 3.1. If there is a large latent heat associated with the transition, this might give the appearance of a limiting temperature. Of course, this would still be a manifestation of the plasma phase.

2. The temperature may rise slowly with energy because of the large density of hadronic states available at higher energies. In a

model proposed many years ago, Hagedorn advanced a density of states for hadrons which had the form[88-89]

$$\sigma(E) = cE^a e^{bE} \tag{46}$$

where $\sigma(E)$ is the density of states at energy E, and a, b and c are parameters. The partition function associated with this density of states,

$$Z(T) = \int dE\ e^{-E/T}\ \sigma(E) \tag{47}$$

clearly has a singularity at

$$T_c = b^{-1}\ . \tag{48}$$

Treated naïvely,[90] this density of states leads to a limiting temperature of about 140 MeV, consistent with the behavior of Fig. 19.

To probe more deeply into the quark plasma, then, one may have to abondon hadronic probes and look at probes with a much longer mean free path in the plasma and the surrounding hadron fluid.[91] Several authors[82-83] have suggested heavy virtual photons, to be observed experimentally as lepton pairs, as being the appropriate tool. These photons would be produced in the plasma phase by the annihilation of quark-antiquark pairs, among other processes, as illustrated in Fig. 20(a). In the hadron phase, they may come from a $\pi\pi$ reaction, as illustrated in Fig. 20(b).

The invariant mass, $\mathcal{M}$, of the $\mu^+\mu^-$ pair clearly will be a function of the temperature: the more energetic the annihilating particles are, on average, the greater the average $\mathcal{M}$ of the pairs. To compare with experiment, one must calculate the event rate in each phase as a function of temperature (taking into account the thermal distribution of energies of the annihilating particles) and then integrate over the

assumed thermal histories of the phases. The calculations, though model dependent, do show[82] a difference in the invariant mass spectrum of $\mu^+\mu^-$ pairs produced in the different phases, particularly at small $\mathcal{M}$. Hence, observation of these lepton pairs should provide a useful signature of the transition.

4. QUARKS IN THE EARLY UNIVERSE

4.1 *The Big Bang Model*

There are at least two areas of astrophysics in which the quark-hadron transition may manifest itself: in the dense cores of heavy stars at temperatures which are low on the nuclear scale, but Δn_B is large, and in the early universe, where the temperatures are much higher and Δn_B is very small. We will not discuss the issue of quark cores in neutron stars, the interested reader being referred to Refs. 42, 46 and 72. Rather, we will concentrate on the role of the transition in the early universe, beginning with a brief review of the Big Bang model. Again, the interested reader is referred to the many technical and popular reviews[92-95] on this subject for greater detail, such as alternate cosmological models and a closer examination of the assumptions involved in the Big Bang model.

There are several observations of present day astronomy which will be used to generate a model for the early universe. The first is the observation[96] of the microwave radiation field which seems to permeate the universe. There do not appear[97] to be any large-scale anisotropies in this microwave radiation, that is, it appears to be associated with the universe as a whole and will therefore be treated here as a relic of the creation of the universe. From measurements made at various

wavelengths, the radiation appears to have a thermal spectrum, with a temperature of close to 3°K, although there are some wavelength regions which deviate from the 3°K spectrum by several standard deviations. Measurements of the spectrum have been made on both the low and high wavelength side of the peak in the spectrum. At present, the photons in this radiation do not interact frequently enough with each other or other material in the universe (compared to the expansion rate of the universe, which we will discuss momentarily) for them to form a thermal distribution. This suggests that the universe previously must have been much hotter than it is today, at least hot enough to form a plasma from the hydrogen in the universe, which would allow the background radiation to be in thermal equilibrium.

The second relevant observation is that the universe appears to be expanding on the large scale. The relationship between the velocity of recession V of a distant object and its distance away R appears to be linear:

$$V = HR \ . \tag{49}$$

The proportionality constant, H, is named after Hubble, who first proposed the relationship on the basis of his analysis[98] of the red shifts of distant galaxies. The current value of H^{-1} is quoted in the range 10-20 billion years. If the universe is currently expanding, then at earlier times it must have been more dense, i.e. the scale of the universe must have been smaller. Since the wavelengths of the microwave radiation will change with the scale of the universe, then at earlier times, the spectrum of this radiation must have been shifted to shorter wavelengths, and hence the radiation possessed a higher temperature.

The Hubble constant itself will be a function of time: it will depend on the energy density U of the universe. General relativity gives the result

$$\frac{1}{R}\frac{dR}{dt} = H = \frac{1}{3}\left(24\pi\, GU/c^2 + 3\Lambda - 9k/R^2\right)^{1/2} \qquad (50)$$

where G is the gravitational constant (we have restored the speed of light, c, for the time being), Λ is the cosmological constant and k is a constant. Assuming that the energy density decreases faster than R^{-2} (it should go like R^{-3} for a matter dominated universe and R^{-4} [$\propto T^4$] for a radiation dominated one) then the term involving k will be dropped. We will also assume that $\Lambda = 0$. Then

$$H \cong \left(\frac{8\pi GU}{3c^2}\right)^{1/2} . \qquad (51)$$

This gives a relation between H and energy density. The relationship between H and t is

$$t_2 - t_1 = \frac{2}{n}\left[H(t_2)^{-1} - H(t_1)^{-1}\right] \qquad (52)$$

where n is the exponent of the power law dependence of U on the reciprocal of the scale of the universe (i.e. $n = 3$ for a matter dominated universe and 4 for a radiation dominated one).

We'll use Eq. (52) in a trivial example. Today's universe is matter dominated ($n = 3$) and has $H^{-1} = (10\text{-}20) \times 10^9$ years. In the very early universe, U was much larger than it is today and hence H was much smaller, or

$$\lim_{t\to 0} H^{-1} = 0 . \qquad (53)$$

Using this limit in Eq. (53), we estimate the age of the universe to be 7 to 13 billion years.

Let us now use Eqs. (51) and (52) to construct a temperature-time

relationship for the early universe. The temperature at which the electron-nuclei (mainly protons and ^{4}He) plasma combined to form neutral atoms is estimated to be (3-4) $\times 10^3$ °K. This yields a time for this event of about 700,000 years (for 3000°K) after the Big Bang. If the clock is wound back further in this radiation dominated universe, to the point at which nuclei are disintegrated by energetic photons ($T \sim 10^9$ °K), the times are of the order of a few minutes after the singularity.

Suppose we take this model seriously and assume that, by and large, the constituents of the universe behave as an ideal gas over much of its early history. Certainly, QCD indicates that this kind of behavior can be expected for the quark-gluon plasma for temperatures in excess of, say, 10^3 MeV (about 10^{13} °K). The time and temperature evolution of the early universe can then be followed at least qualitatively, for temperatures below the Planck mass ($m_{PL} = \sqrt{\hbar c^5/G} = 1.2 \times 10^{19}$ GeV). The Planck mass sets the scale for quantum gravity effects to be important and, as of yet, we can't venture above this temperature with any assurance. For temperatures in the 10^3 to 10^{14} GeV region, it will be assumed that the elementary quanta spectrum consists of:

i) Six flavors of spin 1/2 quarks and antiquarks, each of three colors.

ii) Three massive and three (left handed) massless spin 1/2 leptons and their antiparticles.

iii) Three massive (W^+, W^-, Z^o) and nine massless (1 photon and 8 gluons) spin 1 bosons. (Above temperatures of the order of the electroweak Higgs mass, the spin degrees of freedom of the massive vector bosons may be divided into Higgs scalars and

transverse gauge bosons in the Weinberg-Salam model. This will not affect our counting procedure.)

This gives a value to $\mathcal{N}$ of Eq. (33) of 105 3/4. It is easy to verify, then, that the early universe should follow a temperature history as illustrated in Fig. 21 (which actually included finite masses, but no phase transitions). Several regions which are of importance are indicated in the figure, and these will be discussed in the following section.

The third and last observation which will be used in this Big Bang model of the early universe is that the present day universe appears to be almost entirely matter, and that the amount of antimatter detected in our local galaxy is consistent with what would be produced in the collision of high energy cosmic rays. Further, the baryon number density associated with this matter (which is about 20-24% by weight ^{4}He, the remainder being predominantly hydrogen) is much less than the photon number density, even though the energy density associated with the baryons is much higher. A recent estimate gives[99]

$$n_B/n_\gamma = (3\text{-}5) \times 10^{-10} \tag{54}$$

for the ratio of the number densities. This ratio should be preserved as one winds back the clock: the baryon number density is, at low temperatures, proportional to the baryon mass density which goes like R^{-3}, and the photon number density is proportional to $T^3 \propto R^{-3}$ as well. Properly speaking, one should compare the baryon number density to the entropy density, since the photon number density will change as various species annihilate in the early universe.

At high temperatures, both baryons and antibaryons will be much

more copious since the background radiation will be able to interact via

$$\gamma + \gamma \rightarrow p + \bar{p} \tag{55}$$

for example. At these temperatures, one would expect

$$n_p = n_{\bar{p}} \simeq n_\gamma \tag{56}$$

so that the lhs of Eq. (54) can be replaced by $\Delta n_B/n_B$. The problem of how this slight excess of baryons over antibaryons occurs is one of the more fascinating problems at the interface of cosmology and particle physics.

4.2 *Cosmological Applications of Nuclear and Particle Physics*

As indicated in Fig. 21, there are several temperature regimes at these early times of interest from the nuclear and particle physics point of view. All but the quark-hadron transition will be reviewed in this section. The discussions will be brief, and the interested reader will be referred to the many good reviews available on these topics.

First, we will look at the temperature region around 100 GeV, which is of importance for weak interactions. The Weinberg-Salam model of weak and electromagnetic interactions was first examined at zero temperature, appropriate for current laboratory-based weak interaction phenomena. In this theory,[100] the symmetry of the interaction Lagrangian is broken by the action of a scalar field acquiring a non-vanishing vacuum expectation value. This spontaneous symmetry breakdown has an effect on the particle spectrum of the model: a scalar field and a massless vector field combine to form a massive vector field. In the $SU(2) \otimes U(1)$ theory of weak and electromagnetic interactions, the structure of the Higgs scalar sector is arranged so that only those massless gauge particles which develop into the $W^{\pm}$ and Z^0 bosons gain mass, the photon remaining massless. It has been shown[37] that if the temperature is

raised above a critical value (in the range of the Higgs scalar mass) the symmetry is restored and the gauge bosons become massless. The features of the particle masses in the theory are shown qualitatively in Fig. 22. Hence, above a temperature of a few hundred GeV the W and Z bosons are massless, and the theory undergoes a phase transition[39] as the temperature decreases.

Although this phase transition may not prove to be of great importance in the early universe, a similar transition may have significant consequences at temperatures in the 10^{15} GeV range. This is the temperature scale appropriate to the minimal SU(5) grand unified theory[101] which unites the strong, electromagnetic and weak interactions. The scale is set by examining the variation with q^2 of the running coupling constant associated with the group structure of each of the interactions: SU(3) for the strong, SU(2) for the weak and U(1) for the electromagnetic (labelled α_3, α_2 and α_1 respectively in Fig. 23). The evolution of the effective coupling constants with q^2 shows[102-103] that they seem to converge to a common value at $\sqrt{q^2} \sim 10^{15}$ GeV. There are many models which use this as evidence for the unification of these interactions at this mass scale, the only one which we wish to mention being the minimal model, SU(5). In this model,[104] there are 24 gauge bosons, twelve of which are the familiar gluons, $W^{\pm}$ and Z bosons and photon. The other twelve, dubbed X and Y bosons (six each) have not been observed and have masses on the order of 10^{15} GeV also. The Higgs sector in SU(5) is larger than SU(2) $\otimes$ U(1) as well: at the grand unification scale there are an additional 24 Higgs scalars, 12 of which disappear into the X and Y bosons if the symmetry is broken.

Because SU(5) unites the hadronic and leptonic domains, it is no surprise that the X and Y particles can change quarks into leptons. Examples of some of the couplings allowed are shown in Fig. 24, for the version of SU(5) in which the lightest quarks and leptons are assigned to a common representation. These vertices violate conservation of baryon number, and can lead to proton decay, for example. In Fig. 25(a), the role of the W in the "normal" baryon number conserving β-decay of the neutron is illustrated. This can be contrasted with the baryon number violating decay of the proton shown in Fig. 25(b). Of course the proton will decay only slowly via this mechanism because of the large masses of the X and Y bosons: the effective coupling will be inversely proportional to the X or Y mass squared. Theoretical estimates[104] of the proton lifetime are therefore in the $10^{31\pm2}$ year range, an estimate which should be testable with the new generation of proton decay experiments[105].

One of the ingredients necessary for generating a baryon excess is then present at temperatures in the 10^{15} GeV range: rapid violation of baryon number conservation. Any baryon excess produced at these times will be largely conserved because of the slowness of B-violating interactions at lower temperatures. Two other ingredients necessary to make $\Delta n_B \neq 0$ are also present: a deviation from thermal equilibrium at the phase transition region and CP violation. The actual calculation of the baryon excess is fairly involved and cannot be covered here.[106-109] However, the estimates emerging are certainly in the right ball park, although a gauge group larger than SU(5) may be necessary.[109] Still, there are a great number of problems left outstanding, such as monopole[110-111] production and the role of supercooling,[112-114] which must be solved before this epoch can be said to be understood.

As shown above, the quark-hadron transition occurs at much lower temperatures, in the 200 MeV region for $\Delta n_B = 0$. From Fig. 3, the hadronic density of the universe at this point is well above that of nuclear matter, and it is worthwhile asking whether there will be a phase transition between a hadron liquid and a hadron gas.

To answer this question, a very crude calculation will suffice. If one approximates the NN potential by a square well form as shown in Fig. 26, with a hard core internucleon separation of $2r_o$ and a limit to the attractive well (depth W) of $2r_1$, then one can construct an equation of state for nuclear matter which, at low temperatures, has the van der Waal's form:

$$\left(P + \frac{a}{\tilde{V}^2}\right)(\tilde{V} - b) = T \tag{57}$$

where

$$a = \frac{V_1 - V_o}{2} W \qquad b = \frac{V_o}{2} \qquad V_i = \frac{4\pi}{3}(2r_i)^3 . \tag{58}$$

As before, k has been absorbed into T, and $\tilde{V}$ is the volume per particle. This equation exhibits critical behavior at

$$T_c = \frac{8}{27} \frac{V_1 - V_o}{V_o} W \tag{59}$$

and

$$\tilde{V}_c = \frac{3}{2} V_o . \tag{60}$$

The binding energy per particle is $\frac{27}{8} T_c$. To estimate the hadron liquid-gas phase transition region, a set of parameters ($2r_o$ = 1 fm, $2r_1$ = 1.6 fm and W = 10 MeV) is chosen which does not do too much damage to what we believe the properties of nuclear liquids to be (in other words, this is not a good model for the nuclear matter equation of state, but it will suffice). Because the critical temperature is of the same

order of magnitude as the binding energy per nucleon, we are really only interested in the number density of the early universe when the temperature has dropped down to tens of MeV. By this time, most of the antibaryons will have annihilated, and the number density will follow the curve shown in Fig. 27. One can immediately see that the early universe misses the liquid-gas transition region by a wide margin; there is no phase transition.

The last piece of nuclear physics which should be covered here, and indeed is the justification of the Big Bang model at least for temperatures below the tens of MeV range, is the formation of ^{4}He. The calculation was first performed many years ago,[94] and the formation of ^{4}He and other light nuclei have been intensely investigated since. The reviews of Refs. 115 and 116 serve as a good introduction to this area of study.

As the universe cools through the tens of MeV range, the "exotic" particles such as π's, K's and p's disappear and one is left with a residue of protons and neutrons in a sea of photons, electrons, positrons and neutrinos. The protons and neutrons are kept in equilibrium through reactions such as

$$e^+ + n \rightleftarrows p + \bar{\nu}_e \qquad (61)$$

$$\nu_e + n \rightleftarrows p + e^- \ . \qquad (62)$$

This means that neutrons will decline in abundance relative to protons as the temperature drops into the MeV range, because of the larger neutron mass. The neutron abundance is shown in Fig. 28. At about a second into the life of the universe, neutrons go out of thermal equilibrium and decay freely. There are as yet no nuclei at this temperature because the photon bath is still hot enough to prevent deuterium formation

$$n + p \rightarrow {}^2H + \gamma \qquad (63)$$

which is the first step in forming nuclei. Indeed, ^2H formation does not become favored until the temperature is lowered to about 0.1 MeV, simply because of its small binding energy (1.1 MeV per nucleon). The ^2H so produced at that temperature then rapidly reacts to form ^4He essentially "freezing out" the neutron abundance at 12-13%. The ^4He fraction by weight is double this figure, i.e. 25% or so. This number is in remarkably good agreement with the observed ^4He abundance observed in many different regions of our current universe.

This concludes our brief overview of nuclear and particle physics phenomena in the early universe. The last topic in this paper will be the effect of the relaxation of the confinement constraint and its effect on the free relic quarks produced in the quark-hadron transition.

4.3 *Relic Quarks*

Up until now we have assumed that quarks are permanently confined in hadrons. There is no satisfactory proof that QCD confines quarks although several of the models in Section 2 do show the type of critical behavior which one might expect to find in a theory with confinement. On the experimental side,[15] accelerator based searches for quark production in high energy collisions have not seen evidence for free quarks, putting the free quark mass at a minimum of 4 GeV. The searches for free quarks in nature have yielded contradictory results. Some searches[15] yield free quark to baryon ratios (n_q/n_B) in the 10^{-26} range. However, these searches have come under increasing scrutiny because of the possibility that, for example, the material which went into the search was chemically purified in a way which eliminated (fractionally) charged

particles or that the apparatus discriminated against charged particles. On the other hand, positive results have been reported by some workers[16,117] which can be interpreted as giving a quark concentration in the 10^{-20} quarks/baryon range. Other workers[17,118] have not found positive results.

If free quarks have been observed, then confinement is lost. Several models[18-21] have been advanced by which QCD could be broken (say, with a small gluon mass) leading to the appearance of states which were not color singlets. It is not the purpose of this section to comment on these models, but rather to see what effect the relaxation of confinement has on the production of free quarks in the early universe.

A simple model,[119] which was advanced many years ago, for quark production in the early universe compares the characteristic expansion time of the universe, $t_{exp} \equiv H^{-1}$, with the average reaction time of quarks in the plasma phase

$$t_R^{-1} = n_q \langle \sigma v \rangle \tag{63}$$

where n_q is the quark plus antiquark density and $\langle \sigma v \rangle$ is the thermal average of the product of the quark-quark cross section with the relative velocity of quark pairs. When the average reaction time exceeds t_{exp}, the quarks and antiquarks begin to go out of thermal equilibrium and are frozen out at some density n*. The calculation proceeds as follows:[119-120]

If the expansion rate of the universe is determined by the energy densities of the particles $\gamma, e^+, e^-, \nu_e, \nu_\mu, \nu_\tau$ (and their antineutrinos), then, in the temperature range of interest, Eq. (51) yields

$$T = 1.21\ t_{exp}^{-1/2}\ (\text{MeV}) \tag{64}$$

where t_{exp} is in seconds. In the expression for n_q, we will assume that the quarks are sufficiently massive as to be non-relativistic, and that there are only 2 quark flavors (plus their antiparticles). The cross section will be assumed to have the form

$$\sigma = \sigma_o \left(\frac{c}{v}\right) \tag{65}$$

so that it becomes large at small relative velocities and asymptotically approaches a fixed value as $v \to c$. One then equates $t_{exp} = t_R$ to calculate n^*.

As a test calculation, one can use $\sigma_o = 1$ fm^2 and $m_q = 10$ GeV. The resulting calculation gives the freeze-out temperature of 200 MeV at a time of 4×10^{-5} sec, in the same temperature range as our previous estimates. Further,

$$n^*/n_\gamma = 3.3 \times 10^{-19} \tag{66}$$

leading to $n^*/n_B = 3.3 \times 10^{-10}$ if $n_B/n_\gamma = 10^{-9}$ is used. This ratio is not particularly sensitive to the choice of quark mass (we are really only interested in the exponent), decreasing by about a factor of 3 if the quark mass is lowered to 1 GeV.

Compared to the results of the free quark search, the result is unacceptably large. Part of the problem could be that we have simply underestimated the cross section at small velocities. If a larger power of v is used, or if σ_o is larger, then the quarks will stay in thermal equilibrium longer and hence freeze out at a smaller n^*. A sample calculation of the variation of n^*/n_B with σ_o is shown in Fig. 29. Clearly, in order to get n^*/n_B down into the 10^{-20} range, one needs σ_o in the tevabarn range. This is, of course, the kind of behavior that we expect

from confinement: the quark-quark cross section increases enormously as q^2 decreases, driving n* down.

Wagoner and Steigman[121] have done a more sophisticated calculation than this in which the interquark interaction potential is of the form $V = ar$ up to a maximum value of V of $2m_q$. They can then predict n^*/n_B as a function of the quark mass. For $n^*/n_B \sim 10^{-20}$, the quark mass in this model must lie in the 15-30 GeV range.

Some caution should be exercised in comparing the estimated n^*/n_B as measured, for example, by Fairbank and coworkers, with the relic quarks left over from the early universe. Much of the material which is used in these searches are metals which were not produced in the Big Bang, but rather were produced by nucleosynthesis later in stars. If free quarks were put in a hot enough environment that could overcome some of the coulomb repulsion between the nuclei to which they were bound (assuming that the quarks are bound in fairly tight orbits) then some of the quarks would be able to interact and form normal color singlet hadrons. To illustrate just how strong an effect this might be, the following simple calculation can be performed:

Assuming that there is no coulomb barrier to worry about, one can simply numerically solve the number density equation for a variable rate of reaction (since the quarks will interact less frequently as they combine into hadrons). The results of such a calculation [using $\sigma_{qq} = (c/v)\sigma_o$ and $\sigma_o = 1$ fm^2, as before] are shown in Fig. 30, where $n^*/n_B = 10^{-10}$ at $t = 0$ and n_B is put equal to the average density of the sun. One can see that, over a typical solar lifetime (in the 10^{10} year range) the quark density has decreased drastically. Of course, the inclusion

of a coulomb barrier would significantly moderate this decline. Further, some of the heavy elements may have been produced in much shorter lived stars, and again, the decrease in n^*/n_B will not be as great. The main point to be learned here is that the stellar and terrestial (i.e. chemical) history of the material being examined for free quarks may play a significant role in reducing the free quark density from what remains after the quark-hadron transition.

5. SUMMARY

In the above we have seen evidence that at high densities the constituents of hadrons may become free to propagate through the hadronic medium. Although a complete theory of the strong interaction which is calculable at all coupling strengths is not yet available, nevertheless several models which approximate the characteristics which we believe the complete theory should have, do show a phase transition from hadronic matter to a quark-gluon plasma phase. The evidence includes a breakdown in finite temperature perturbative QCD at a temperature in the hundreds of MeV range, and discontinuous behavior in the specific heat of a pure gauge theory on the lattice. Models which give up some rigor in favor of better behavior around the phase transition region, such as the mean-field-like model of Section 2.3 or the explicit two phase models of Section 2.4, allow one to estimate the thermodynamic limits of the quark-gluon phase. These estimates yield a temperature of 200-300 MeV for the transition at $\Delta n_B = 0$, and $n_B = 5\text{-}20\ n_o$ for the transition at $T = 0$. These values are of the same order as what is obtained from very simple geometrical considerations.

How this transition will manifest itself experimentally is a more

difficult problem. The most likely type of experiment would involve the collision of two relativistic heavy nuclei in the hope that there will be a sufficient number of hadronic interactions that a thermally equilibrated system will be formed. Of course, the lifetime of such a system will be on the hadronic time scale, 10^{-23} or 10^{-22} seconds. The kinetic energy per nucleon for a heavy ion incident upon a stationary target may only have to be in the few GeV region in order to access the kind of temperatures and densities associated with the phase transition. However, if there is a substantial latent heat involved in changing phase, then the incident heavy ion will have to be much more energetic, perhaps in the 10-20 GeV per nucleon range.

The energy spectrum of hadrons produced in heavy ion reactions has long been used as a means of estimating the temperature of the source of those hadrons. Because any hadrons emitted from the quark plasma are mainly going to come from the surface boundary of the plasma with a cooler envelope of hadrons, the temperature which these emitted hadrons would measure will most likely be the phase transition temperature (assuming that they can get through the remaining hadronic envelope without cooling substantially). Hence, as a function of increasing bombarding energy, one would expect to see the hadronic temperature rise until the transition temperature is reached and then remain roughly static. Such behavior is observed experimentally, although there may be several alternate explanations for it, such as the inability of the incident heavy ion to increase the temperature further because of changing nucleon-nucleon dynamics.

A better means of measuring the plasma would be to use a probe

which has a much longer mean free path in both the plasma and hadronic phases. Massive virtual photons, manifesting themselves by producing lepton pairs of large invariant mass, have been suggested as such a probe. Evaluation of quantities such as the invariant mass spectrum of these pairs in the presence and absence of the quark phase are difficult owing to the need to take into account, for example, the thermal distributions of particles of the phases. Nevertheless, the calculations done so far are encouraging.

Other areas in which the plasma phase may play a role are in the cores of heavy stars and in the study of the early universe. Only the latter area was addressed in these lectures. The most interesting aspect of the role of this transition is not so much the transition to a hadron phase with confined quarks, but rather the consequences of the relaxation of the confinement constraint. If quarks are not permanently confined to hadrons, but rather are simply deeply bound, then there should be a residue of them left over from their condensation into hadrons which occurred some 10^{-5} seconds after the Big Bang. A simple model for the quark-quark interaction cross section leads to an estimated abundance of relic quarks compared to present day baryon number density of 10^{-9}, with the exponent being highly model dependent. Although many searches for free quarks have not turned up positive evidence for their existence, those searches which do yield positive results (for the existence of fractional charge, which will be treated as meaning free quarks here) can naïvely be interpreted as giving a quark to baryon ratio of something in the 10^{-20} range. This is, of course, much less than that predicted in a simple Big Bang calculation.

Two things could explain this discrepancy, if in fact the positive results are real. The first is that the quark-quark interaction cross section is much larger than the calculation has naïvely assumed, particularly at low relative velocities. This would correspond to a more "confinement-like" potential which, in turn, would lead to a lower free quark abundance. The second explanation has to do with the nature of the material in which the fractional charges have been observed—niobium. The main elemental products of the Big Bang are hydrogen, helium and other very light elements. Metals like niobium are produced from this Big Bang debris through nucleosynthesis in stars. In a hot stellar environment over at least hundreds of millions of years, the free quarks may have a large probability of finding each other and forming color singlet hadrons. It is difficult to estimate just how strong an effect this will be until one knows how a quark binds to a nucleus; that is, coulomb repulsion between nuclei may inhibit quark recombination. However, if the stellar temperature were hot enough to overcome coulomb effects, then the present day free quark density in heavy metals could be much lower than that of the early universe. Accelerator based quark searches at higher energy, searches for quarks in light elements, and an understanding of the chemistry and physics of quark-nucleus systems will help resolve this question.

Note added in proof: Since these lectures were given (January, 1982) significant progress has been made on the problem of incorporating fermions into lattice gauge theories. See, for example, J. Engels, F. Karsch and H. Satz, Phys. Lett. 113B, 398 (1982).

Acknowledgments

The author wishes to thank the faculty of the Physics Department at Michigan State University for their warm hospitality during his stay at the Cyclotron Laboratory when these lectures were given. He also wishes to thank R.M. Woloshyn and R.V. Wagoner for stimulating discussions about the problems dealt with in these notes. Lastly, the Natural Sciences and Engineering Research Council of Canada provided financial support for this work.

References

1. M. Gell-Mann, Phys. Lett. 8, 214 (1964).
2. G. Zweig, CERN Reports Nos. TH-401 and TH-412, 1964 (unpublished); *Proceedings of the International School of Physics "Ettore Majorana"*, Erice, Italy, 1964, ed. by A. Zichichi (Academic, New York, 1965) p. 192.
3. R.H. Dalitz in *Proceedings of the Oxford International Conference on Elementary Particles* (Rutherford High Energy Laboratory, 1966) p. 157.
4. Many examples are listed in F.E. Close, *An Introduction to Quarks and Partons* (Academic, New York, 1979).
5. R.P. Feynman, *Photon-Hadron Interactions* (Benjamin, New York, 1972).
6. J.J. Aubert *et al.*, Phys. Rev. Lett. 33, 1404 (1974).
7. J.E. Augustin *et al.*, Phys. Rev. Lett. 33, 1406 (1974).
8. J.L. Rosner, in *Techniques and Concepts of High Energy Physics*, ed. by T. Ferbel (Plenum, New York, 1981) p. 1.
9. A. De Rujula, H. Georgi and S.L. Glashow, Phys. Rev. D12, 147 (1975).
10. N. Isgur and G. Karl, Phys. Rev. D18, 4187 (1978).

11. W. Buchmüller and S-H.H. Tye, in *Perturbative Quantum Chromodynamics*, D.W. Duke and J.F. Owens, eds., (American Institute of Physics, New York, 1981) p. 370.

12. H. Georgi and H.D. Politzer, Phys. Rev. D9, 416 (1974).

13. D.J. Gross and F. Wilczek, Phys. Rev. D9, 980 (1974).

14. A. De Rujula, H. Georgi and H.D. Politzer, Phys. Rev. D10, 2141 (1974).

15. For a review, see L.W. Jones, Rev. Mod. Phys. 49, 717 (1977).

16. G.S. Larue, W.M. Fairbank and A.F. Hebard, Phys. Rev. Lett. 38, 1011 (1977).

17. G. Gallinaro, M. Marinelli and G. Morpugo, Phys. Rev. Lett. 38, 1255 (1977).

18. A. De Rujula, R.C. Giles and R.L. Jaffe, Phys. Rev. D17, 285 (1978).

19. H. Georgi, Phys. Rev. D22, 225 (1980); A. De Rujula, R.C. Giles and R.L. Jaffe, Phys. Rev. D22, 227 (1980).

20. E.W. Kolb, G. Steigman and M.S. Turner, Phys. Rev. Lett. 47, 1357 (1981).

21. R. Slansky, T. Goldman and G.L. Shaw, Phys. Rev. Lett. 47, 887 (1981).

22. G. Baym, Physica 96A, 131 (1979).

23. V.K.S. Shante and S. Kirkpatrick, Adv. Phys. 20, 325 (1971).

24. S. Kirkpatrick, Rev. Mod. Phys. 45, 574 (1973).

25. For a brief review of Bravais lattices, see, for example, C. Kittel, *Introduction to Solid State Physics* (Wiley, New York, 1953).

26. F. Karsch and H. Satz, Phys. Rev. D21, 1168 (1980).

27. See, for example, H.D. Politzer, Phys. Reports 14C, 129 (1974).

28. This, and the more exact argument follow along the lines developed by R.D. Field in *Quantum Chromodynamics*, W. Frazer and F. Henyey eds.,

(American Institute of Physics, New York, 1979) p. 97. The interested reader is referred to these proceedings for detailed applications of Q.C.D.

29. For a review, see W. Marciano and H. Pagels, Phys. Rep. 36C, 137 (1978).
30. J.L. Richardson, Phys. Lett. 82B, 272 (1979).
31. H. Georgi and H.D. Politzer, Phys. Rev. D14, 1829 (1976).
32. See, for example, R.L. Stuller, Phys. Rev. D13, 513 (1976).
33. J.I. Kapusta, Nucl. Phys. B148, 461 (1979).
34. D. Kirzhnits and A. Linde, Phys. Lett. 42B, 471 (1972).
35. C.W. Bernard, Phys. Rev. D9, 3312 (1974).
36. L. Dolan and R. Jackiw, Phys. Rev. D9, 3320 (1974).
37. S. Weinberg, Phys. Rev. D9, 3357 (1974).
38. B.J. Harrington and A. Yildiz, Phys. Rev. Lett. 33, 324 (1974).
39. For a review, see A. Linde, Rep. Prog. Phys. 42, 389 (1979).
40. N.J. Snyderman, SLAC report SLAC-PUB-2636.
41. J.C. Collins and M.J. Perry, Phys. Rev. Lett. 34, 1353 (1975).
42. P.D. Morley and M.B. Kislinger, Phys. Rep. 51, 63 (1979) and references therein.
43. B.A. Freedman and L.D. McLerran, Phys. Rev. D16, 1130,1147,1169 (1977).
44. V. Baluni, Phys. Rev. D17, 2092 (1978).
45. D.J. Gross, R.D. Pisarski and L.G. Yaffe, Rev. Mod. Phys. 53, 43 (1981) and references therein.
46. E.V. Shuryak, Phys. Rep. 61, 71 (1980) and references therein; E.V. Shuryak, Zh. Eksp. Teor. Fiz. 74, 408 (1978) [Sov. Phys. JETP 47, 212 (1978)].
47. M. Chemtob, Nucl. Phys. B184, 497 (1981).
48. C.-G. Källman, Phys. Lett. 85B, 392 (1979).

49. N. Bilic and D.E. Miller, Phys. Rev. D23, 934 (1981).

50. K. Wilson, Phys. Rev. D10, 2445 (1974).

51. J. Kogut and L. Susskind, Phys. Rev. D11, 395 (1975).

52. M. Weinstein in *Particles and Fields*, D.H. Boal and A.N. Kamal eds., (Plenum, New York, 1978) p. 321.

53. M. Creutz, Rev. Mod. Phys. 50, 561 (1978).

54. L. Susskind in *Quantum Chromodynamics*, W. Frazer and F. Henyey eds., (American Institute of Physics, New York, 1979) p. 243.

55. See P. Goddard, J. Goldstone, C. Rebbi and C.B. Thorn, Nucl. Phys. B56, 109 (1973) and references therein.

56. J.S. Kang and H.J. Schnitzer, Phys. Rev. D12, 841 (1975).

57. P.D.B. Collins and E.J. Squires, *Regge Poles in Particle Physics* (Springer-Verlag, Berlin, 1968).

58. M. Creutz, Phys. Rev. D21, 2308 (1980).

59. For a synopsis including higher $SU(N)_c$, see M. Creutz in *Perturbative Quantum Chromodynamics*, D.W. Duke and J.F. Owens, eds., (American Institute of Physics, 1981) p. 459.

60. J. Kuti, J. Polónyi and K. Szlachányi, Phys. Lett. 98B, 199 (1981).

61. L.D. McLerran and B. Svetitsky, Phys. Lett. 98B, 195 (1981).

62. J. Engels, F. Karsch, H. Satz and I. Montvay, Phys. Lett. 101B, 89 (1981).

63. I. Montvay and E. Pietarinen, University of Helsinki Report HU-TFT-82-8.

64. C.G. Callen Jr., R.F. Dashen and D.J. Gross, Phys. Rev. D20 3279 (1979).

65. C.G. Callen Jr., R.F. Dashen and D.J. Gross, Phys. Rev. Lett. 44 4351 (1980).

66. K.A. Olive, Nucl. Phys. B190 [FS3], 483 (1981).

67. D.H. Boal, J. Schachter and R.M. Woloshyn, TRIUMF Report TRI-PP-82-14.

68. For a mean field theory of nuclear matter, see J.D. Walecka, Phys. Lett. 59B, 109 (1975) and R.A. Freedman, Phys. Lett. 71B, 369 (1977). These calculations are both different and formally more rigorous than the approach described in this lecture.

69. W. Celmaster and F.S. Henyey, Phys. Rev. D18, 1688 (1978).

70. For a discussion of the possibility of different color weightings in various models, see H. Suura, Phys. Rev. D17, 469 (1978), 20, 1412 (1979).

71. F. Karsch and H. Satz, Phys. Rev. D22, 480 (1980).

72. G. Baym and S.A. Chin, Phys. Lett. 62B, 241 (1976).

73. A. Chodos *et al.*, Phys. Rev. D9, 3471 (1974).

74. T. De Grand *et al.*, Phys. Rev. D12, 2060 (1975).

75. J.D. Walecka, Ann. Phys. 83, 491 (1974).

76. S.A. Chin, Phys. Lett. 78B, 552 (1978).

77. G. Chapline and M. Nauenberg, Phys. Rev. D16, 450 (1977).

78. J. Kuti, B. Lukacs, J. Polonyi and K. Szlachanyi, Phys. Lett. B95, 75 (1980).

79. E. Alvarez, Phys. Rev. D23, 1715 (1981). See also E. Alvarez and R. Hakim, Phys. Rev. D19, 1696 (1979).

80. For a review, see S. Nagamiya and M. Gyulassy in *Advances in Nuclear Science*, J.W. Negele and E. Vogt eds., (Plenum, New York, in press).

81. K.A. Olive, Phys. Lett. 89B, 299 (1980).

82. G. Domokos and J.I. Goldman, Phys. Rev. D23, 203 (1981).

83. K. Kajantie and H.I. Miettinen, Helsinki University Report HU-TFT-81-7.

84. K.K. Gudima and V.D. Toneev, Dubna Report E2-12644 (1979). See also R. Anishetty, P. Koehler and L.D. McLerran, Phys. Rev. D22, 2793 (1980).

85. The argument, and the experimental evidence for it, is reviewed in Ref. 80.

86. D.K. Scott, Michigan State University Report MSUCP-364.

87. G.D. Westfall *et al.*, Michigan State University Report.

88. R. Hagedorn, Suppl. Nuovo Cim. 3, 147 (1965).

89. See also S. Frautschi, Phys. Rev. D3, 2821 (1971).

90. This interpretation of the exponential densities of states has been examined more thoroughly by, for example, N. Cabbibo and G. Parisi, Phys. Lett. 59B, 67 (1975).

91. For a discussion of what one can learn from hadronic abundance ratios, see Ref. 81. The effects of the quark plasma on the rapidity distribution of secondaries is discussed in F. Halzen and H.C. Liu, Phys. Rev. D25, 1842 (1982).

92. J. Silk, *The Big Bang* (Freeman, San Francisco, 1980).

93. S. Weinberg, *The First Three Minutes* (Basic Books, New York, 1977).

94. P.J.E. Peebles, *Physical Cosmology* (Princeton University Press, Princeton, 1971).

95. R.V. Wagoner in *Physical Cosmology, Les Houches, Session XXXII, 1979*, R. Balian, J. Audouze and D.N. Schramm, eds. (North Holland, New York, 1980).

96. A.A. Penzias and R.W. Wilson, Astrophys. J. 142, 419 (1965).

97. G.F. Smoot, M.V. Gorenstein and R.A. Muller, Phys. Rev. Lett. 39, 898 (1977).

98. See E. Hubble, *The Realm of the Nebulae* (Yale University Press, New Haven, 1936; reprinted by Dover Publications, Inc., New York, 1958).

99. K.A. Olive, D.N. Schramm, G. Steigman, M.S. Turner and J. Yang, Astrophys. J. 246, 557 (1981).

100. For a review, see J.C. Taylor, *Gauge Theories of Weak Interactions* (Cambridge University Press, Cambridge, 1976).

101. H. Georgi and S.L. Glashow, Phys. Rev. Lett. 32, 438 (1974).

102. A.J. Buras, J. Ellis, M.K. Gaillard and D.V. Nanopoulos, Nucl. Phys. B135, 66 (1978).

103. H. Georgi, H. Quinn and S. Weinberg, Phys. Rev. Lett. 32, 451 (1974).

104. For a review, see P. Langacker, Phys. Rep. 72C, 185 (1981).

105. *The Existing Limit to the Lifetime is $\sim 10^{30}$ Years.* See F. Reines and M.F. Crouch, Phs. Rev. Lett. 32, 493 (1974).

106. S. Weinberg, Phys. Rev. Lett. 42, 850 (1979).

107. M.S. Turner, NSF Institute for Theoretical Physics Report NSF-ITP-81-85 (1981).

108. E.W. Kolb and S. Wolfram, Nucl. Phys. B172, 224 (1980).

109. J.A. Harvey, E.W. Kolb, D.B. Reiss and S. Wolfram, Caltech Report CALT-68-850 (1981).

110. P. Langacker and S-Y. Pi, Phys. Rev. Lett. 45, 1 (1980).

111. T.W.B. Kibble, Phys. Rep. 67C, 183 (1980).

112. J.D. Barrow and M.S. Turner, Nature 292, 35 (1981).

113. A.H. Guth, Phys. Rev. D23, 347 (1981).

114. G. Steigman to appear in the *Proceedings of the Europhysics Study Conference: Unification of the Fundamental Interactions-II* (1981).

115. D.N. Schramm and R.V. Wagoner, Ann. Rev. Nucl. Sci., 27, 37 (1977).

116. S.M. Austin, Prog. Nucl. Part. Phys. 7, 1 (1981).

117. G.S. Larue, W.M. Fairbank and J.D. Phillips, Phys. Rev. Lett. 42, 142,1019(E) (1979).

118. V.B. Braginsky, L.S. Kornienko and S.S. Poloskov, Phys. Lett. 33B, 613 (1970).

119. Ya.B. Zeldovich, L.B. Okun and S.B. Pikelner, Usp. Fiz. Nauk 87, 113 (1965) [Sov. Phys. Usp. 8, 702 (1966)].

120. S. Frautschi, G. Steigman and J. Bahcall, Astrophys. J. 175, 307 (1972).

121. R.V. Wagoner and G. Steigman, Phys. Rev. D20, 825 (1979).

Table 1. Density of lattice points per unit volume for touching spheres of radius r_o.

Lattice type	Abbreviation	Density
Simple cubic	sc	$(8r_o^3)^{-1}$
Body-centered cubic	bcc	$2/(4r_o/\sqrt{3})^3$
Face-centered cubic	fcc	$(4\sqrt{2}r_o^3)^{-1}$

Table 2. Estimated constituent quark masses from $J^P = 1^-$ mesons. These masses are not used in the detailed calculations presented in this paper.

Name	Symbol	Mass (MeV)
up	u	385
down	d	385
strange	s	510
charm	c	1550
beauty	b	4700
truth	t	?

Figure Captions

1. Quark-antiquark potential from Ref. 11, Fig. 1. Shown is an estimated range of several models given in Ref. 11. The potentials have been made to coincide at 0.5 fm. Estimated normalization uncertainty is shown.
2. Close packed rigid spheres of baryons and mesons.
3. Summed hadronic densities for an ideal gas of hadrons. Zero net baryon number.
4. Abundances of particular hadronic species as a percentage of total hadrons. Non-interacting hadrons at zero net baryon number have been assumed.
5. Quark (or antiquark) number density as a function of temperature for a quark of mass 1.5 GeV. A factor of 6 for spin and color is included.
6. Feynman rules for Q.C.D. The solid and wavy lines are quarks and gluons respectively. The dotted lines are ghost particles: fictitious particles which must be introduced in the calculations but do not manifest themselves physically.
7. Screening of electric (a) and color (b) charge in QED and QCD. Antiscreening of color charge in QCD (c). The labels R and B denote color charges. From Ref. 28.
8. Examples of graphs of order g (a), g^3 (b).
9. Behavior of $\tilde{\alpha}_s(Q^2)$ (dashed curve) and $\tilde{\alpha}'_s(Q^2)$ (solid curve) as a function of Q^2 for $\Lambda = 500$ MeV.
10. Effective mass of the u-quark as found in the QCD calculation of Ref. 33.

11. Ratio of $-P_2/P_0$ and P_3/P_0 in a perturbative QCD calculation (following Ref. 33).

12. Behavior of the rhs of Eq. (23) in the background potential model as a function of n_i for three flavors of massless quarks. The temperatures used are 319 MeV (high), 308 MeV (critical) and 295 MeV (low).

13. Quark-hadron transition region for the effective mass (dashed curve) and background potential (full curve) models. The numerical calculation did not behave properly above $\Delta n_B \approx 0.5$ fm^{-3}, so the numerical result was simply extrapolated to the estimate from Eq. (38).

14. Up quark mass in the effective mass calculation at $\mu = 0$.

15. Ideal gas pressures for the quark-gluon phase (full curve) and the hadron phase (dashed curve). The photon and lepton contribution to each phase is included, but the hadron phase contains only those hadrons with mass less than 1.5 GeV.

16. Energy density vs baryon number density relation estimated for a collision of two equal mass nuclei from the simple model of Section 3.1 (full curve). The cross marks on the curve indicate the kinetic energy per nucleon of the incident heavy ion in the laboratory frame. The cross hatched region represents the phase transition boundary of the model in Section 2.3.

17. Qualitative features of the temperature of an expanding fireball as a function of radial distance.

18. Qualitative features of the temperature of a quark plasma formed in a heavy ion collision.

19. Estimated fireball temperatures (determined hadronically).
20. Possible mechanisms for production of massive $\mu^+\mu^-$ pairs in the quark phase (a) and hadron phase (b).
21. Temperature evolution of the early universe for ideal gas constituents.
22. Qualitative temperature dependence of the W, photon and Higgs scalar masses. From Ref. 37.
23. Qualitative behavior of the running coupling constants α_i [i = 1 for U(1), 2 for SU(2) and 3 for SU(3)] as a function of $\sqrt{q^2}$.
24. Couplings of the X and Y bosons to quarks and leptons.
25. The "normal" β-decay of the neutron is shown in (a). Possible baryon number violating decays of the proton are shown in (b).
26. Square well approximation for NN interaction.
27. Estimated nucleon number density for the early universe compared to the phase transition region estimated for a nuclear liquid.
28. Estimated neutron abundance in the first few minutes of the universe. It is not until the temperature has dropped to about 0.1 MeV that neutrons can react to form nuclei, freezing out the neutrons at about 12% abundance.
29. Variation of the relic quark to baryon density as a function of σ_o.
30. Evolution of n^*/n_B with time in a hot star ($\sigma_o = 1$ fm^2), assuming no coulomb barrier.

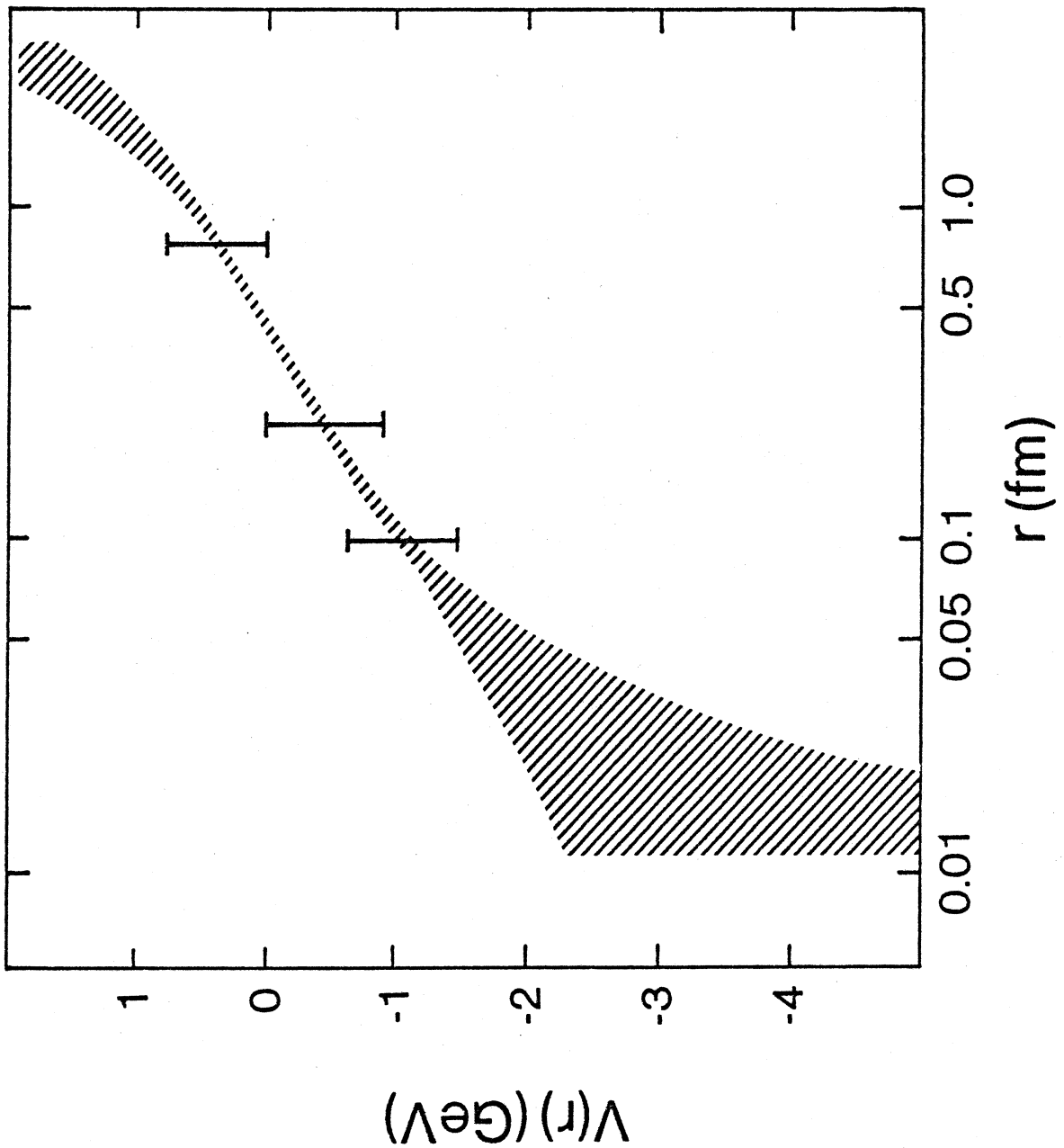

FIG. 1

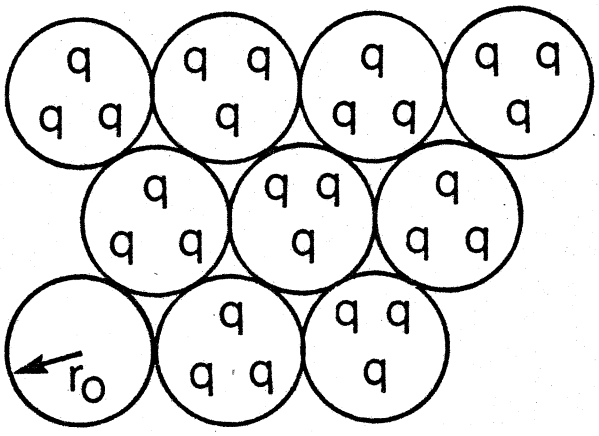

BARYONS

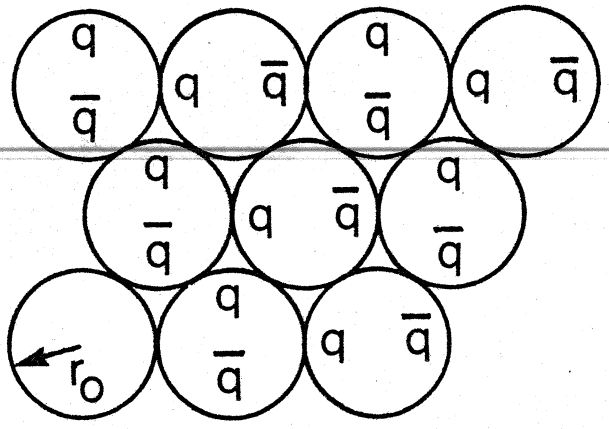

MESONS

FIG. 2

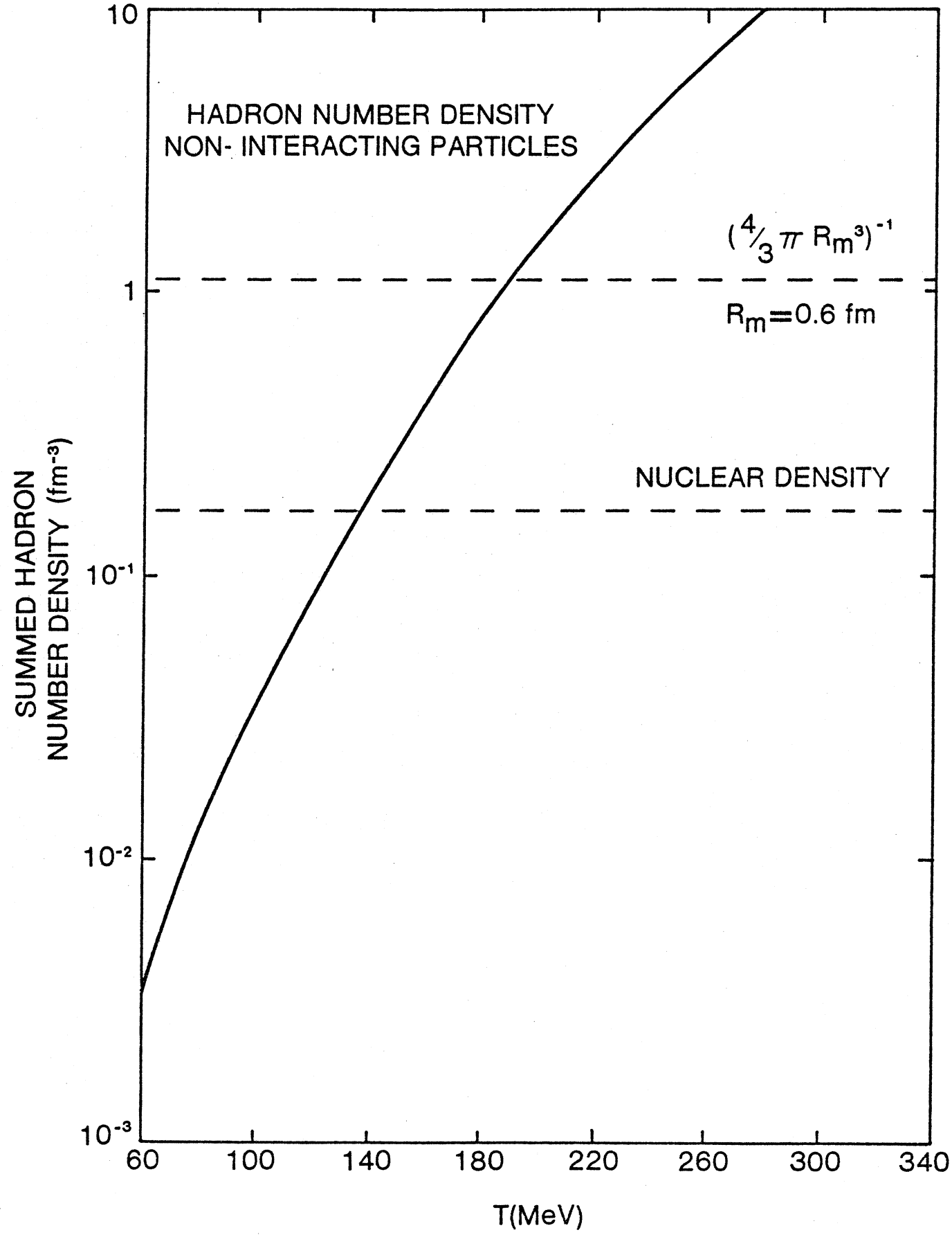
HADRON NUMBER DENSITY
NON- INTERACTING PARTICLES
$(\frac{4}{3}\pi R_m^3)^{-1}$
R_m=0.6 fm
NUCLEAR DENSITY
SUMMED HADRON NUMBER DENSITY (fm^{-3})
10
1
10^{-1}
10^{-2}
10^{-3}
60
100
140
180
220
260
300
340
T(MeV)

FIG. 3

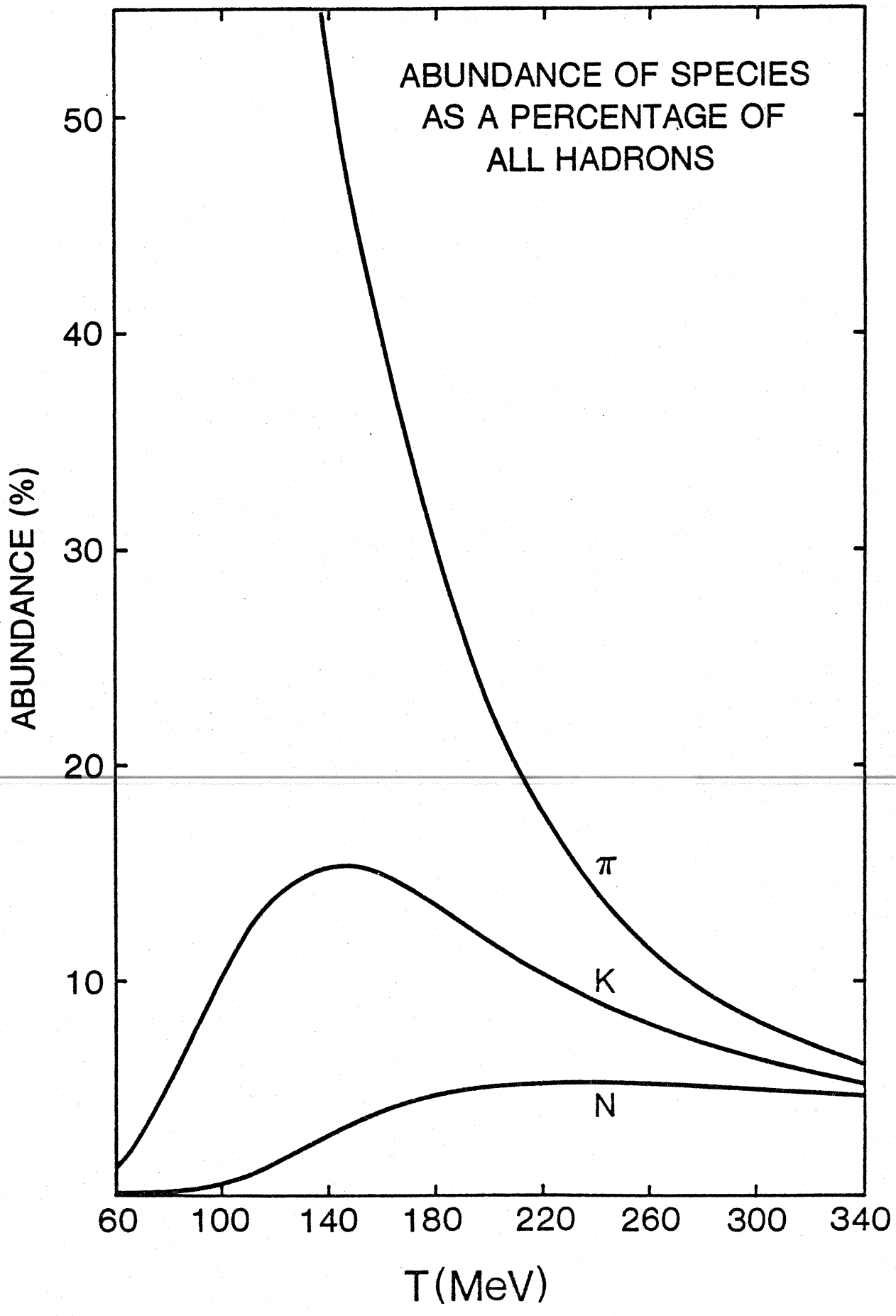
ABUNDANCE OF SPECIES
AS A PERCENTAGE OF
ALL HADRONS
ABUNDANCE (%)
50
40
30
20
10
π
K
N
60
100
140
180
220
260
300
340
T(MeV)

FIG. 4

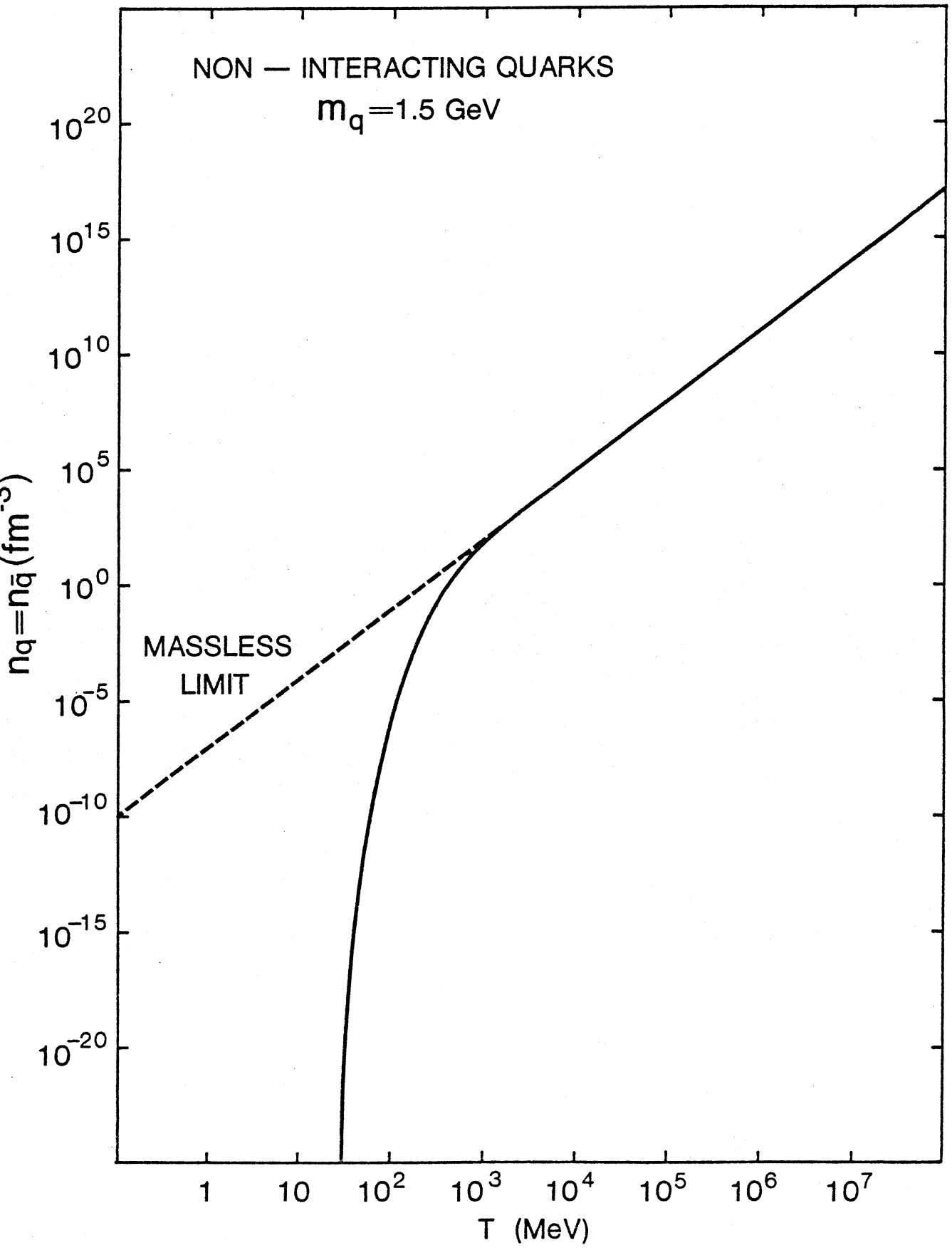
NON — INTERACTING QUARKS
m_q=1.5 GeV
10^{20}
10^{15}
10^{10}
10^{5}
10^{0}
10^{-5}
10^{-10}
10^{-15}
10^{-20}
$n_q=n_{\bar{q}}$ (fm^{-3})
MASSLESS
LIMIT
1
10
10^2
10^3
10^4
10^5
10^6
10^7
T (MeV)

FIG. 5

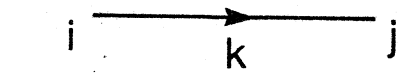

$$S_o = \frac{-\delta_{ij}}{\not{k}-m}$$

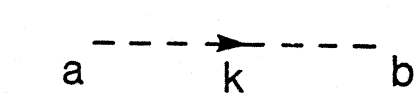

$$W_o = \frac{-\delta_{ab}}{k^2}$$

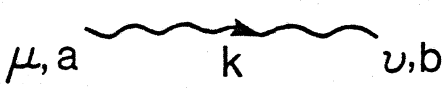

$$D_o = \frac{\delta_{ab}}{k^2}\left[g_{\mu\upsilon} - (1-\alpha)\frac{k_\mu k_\upsilon}{k^2}\right]$$

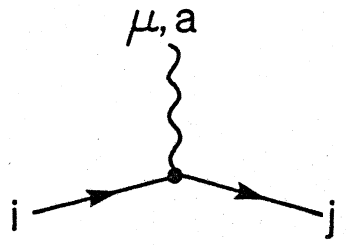

$$\Gamma_o^Q = -g\gamma^\mu \tau^a_{ij}$$

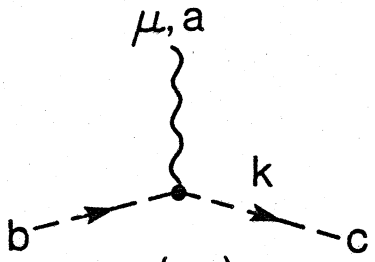

$$\Gamma_o^G = -ig\ f_{abc}\ k_\mu$$

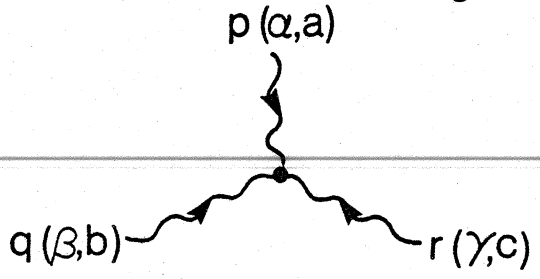

$$\Gamma^V_{o,3} = -igf_{abc}\left[g_{\beta\gamma}\ (q-r)_\alpha + g_{\alpha\beta}(p-q)_\gamma + g_{\gamma\alpha}\ (r-p)_\beta\right]$$

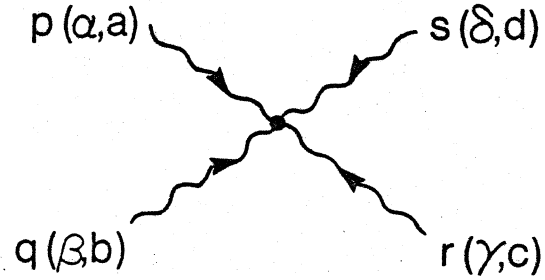

$$\Gamma^V_{o,4} = -g^2\Big[f_{ade}f_{ebc}\,(g_{\alpha\beta}g_{\delta\gamma} - g_{\alpha\gamma}g_{\delta\beta}) + f_{abe}f_{edc}\,(g_{\alpha\delta}g_{\beta\gamma} - g_{\alpha\gamma}g_{\delta\beta}) + f_{ace}f_{edb}\,(g_{\alpha\delta}g_{\beta\gamma} - g_{\alpha\beta}g_{\delta\gamma})\Big]$$

FIG. 6

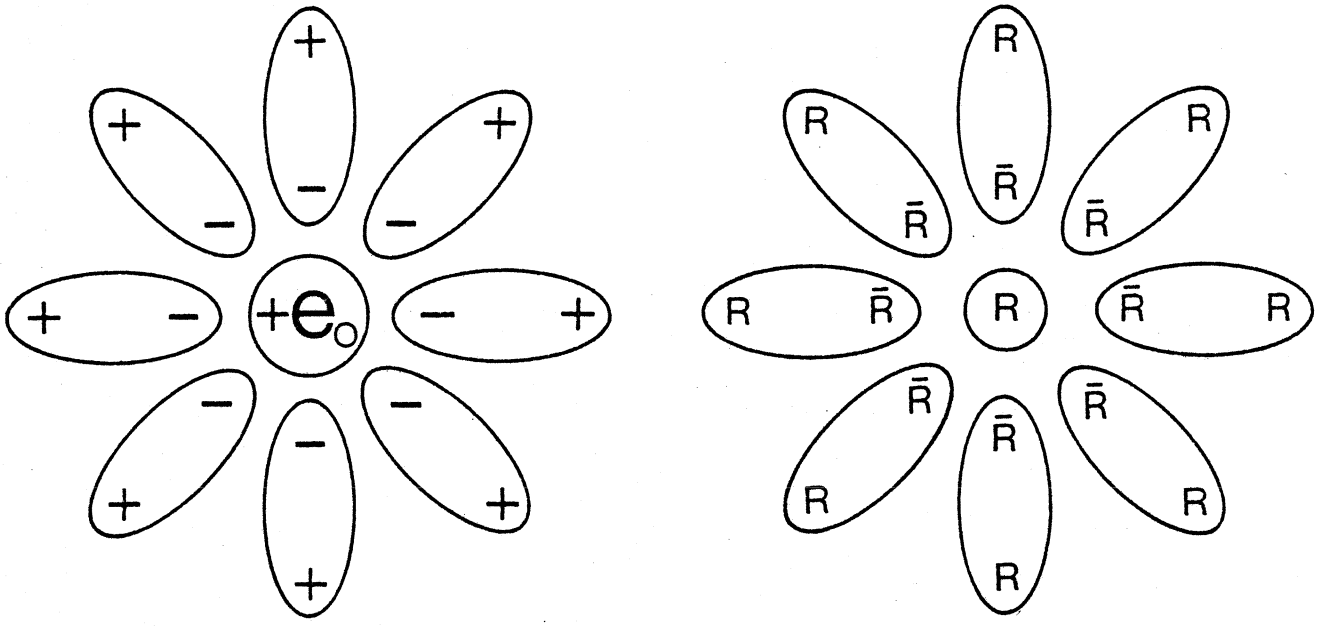

(a) (b)

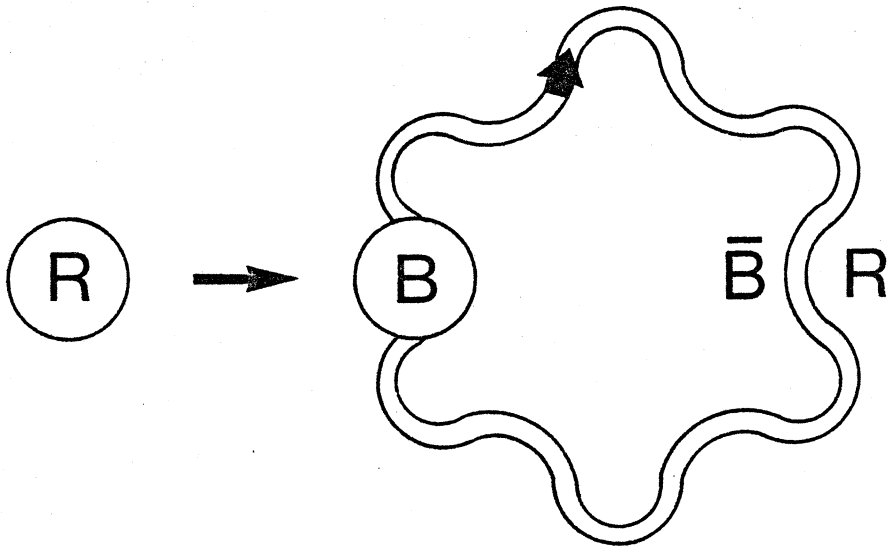

(c)

FIG. 7

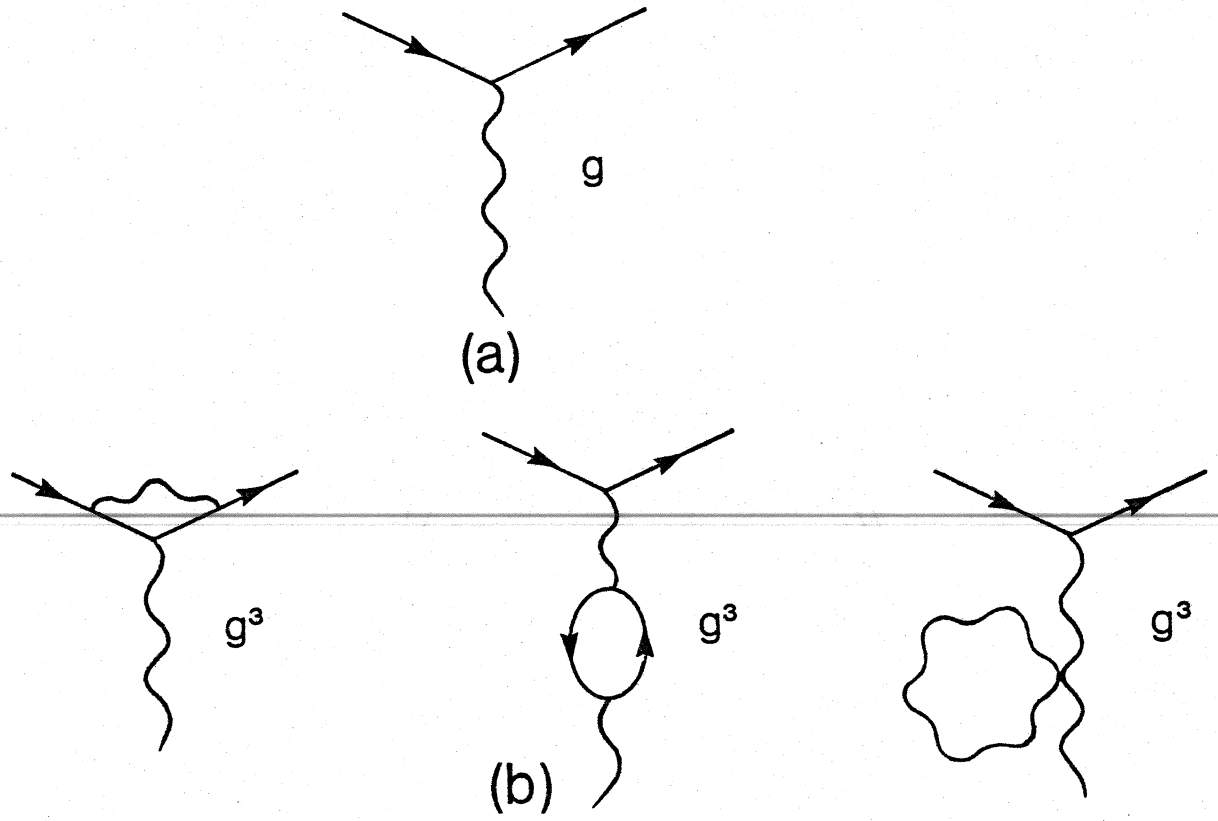

FIG. 8

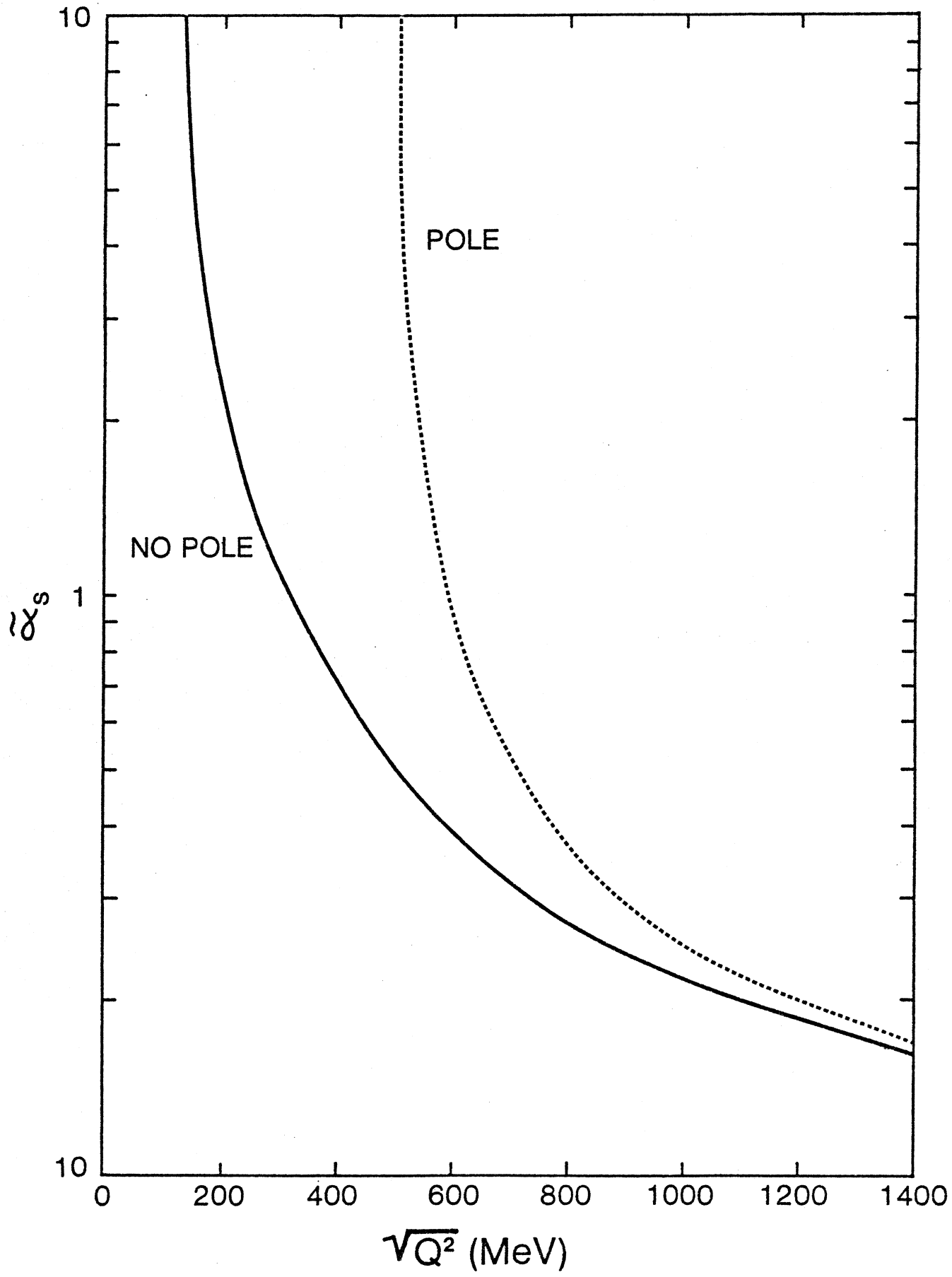
10
1
10
$\tilde{\alpha}_s$
POLE
NO POLE
0
200
400
600
800
1000
1200
1400
$\sqrt{Q^2}$ (MeV)

FIG. 9

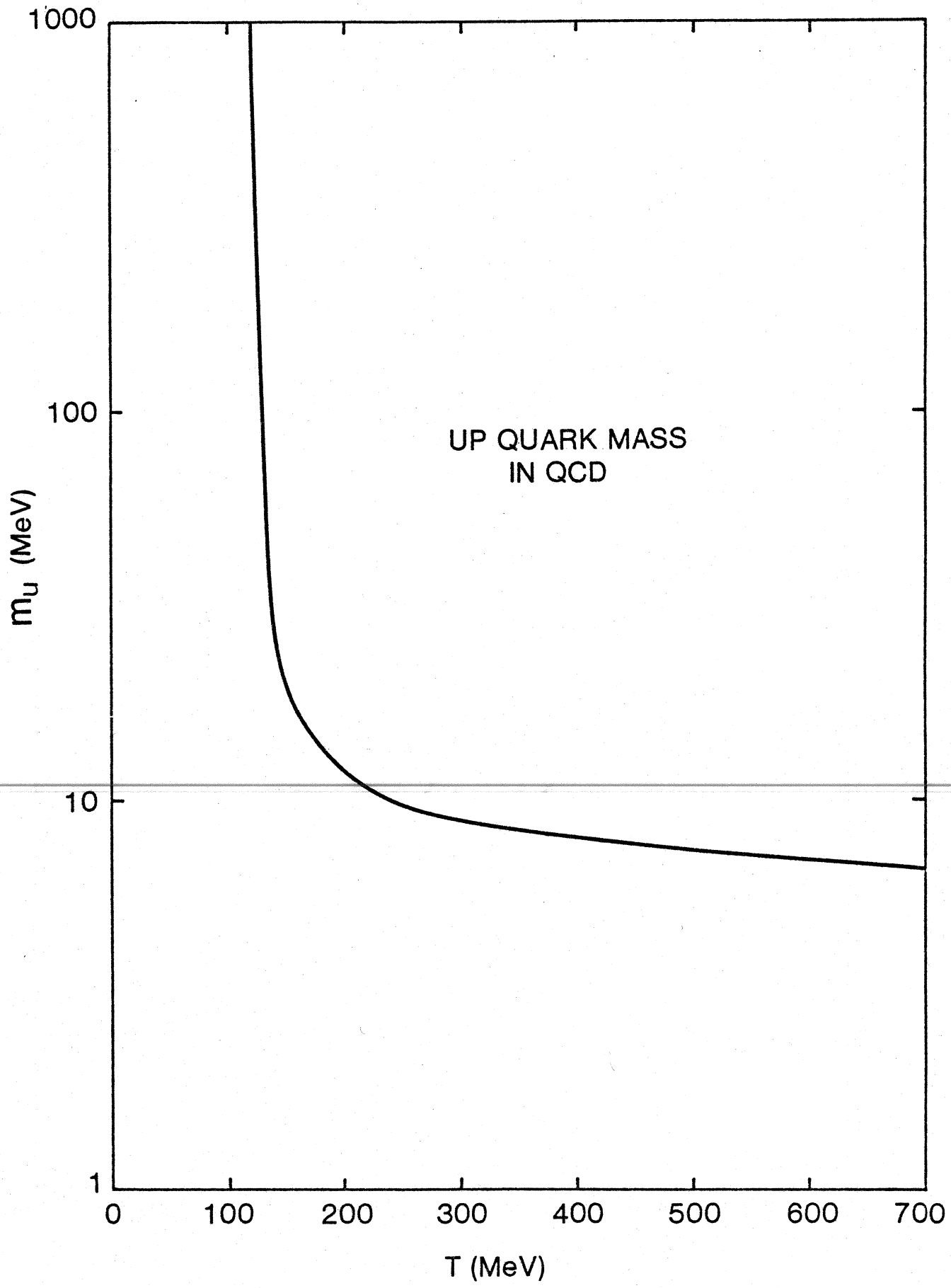
1000
100
10
1
m_u (MeV)
UP QUARK MASS
IN QCD
0
100
200
300
400
500
600
700
T (MeV)

FIG. 10

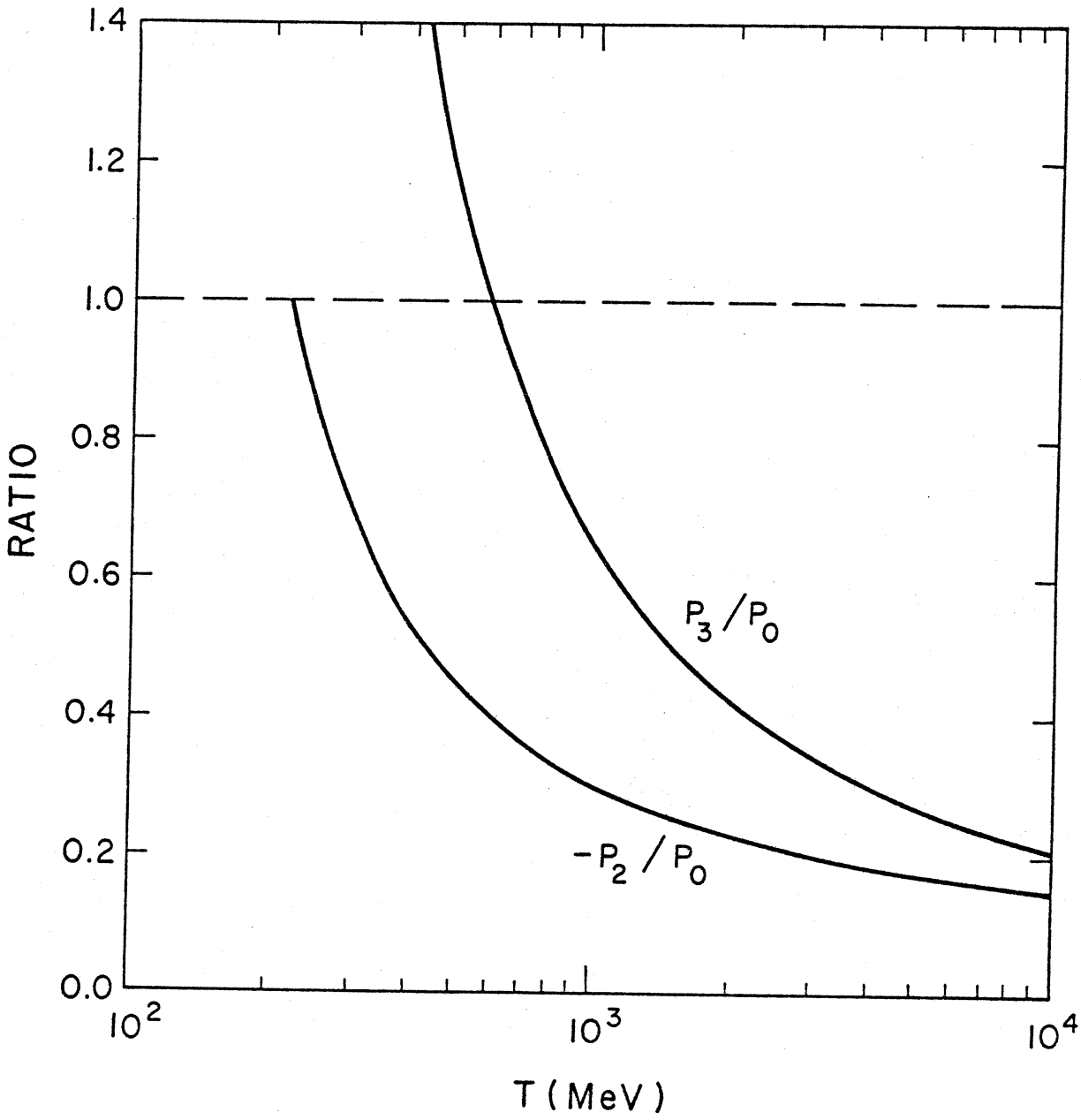

FIG. 11

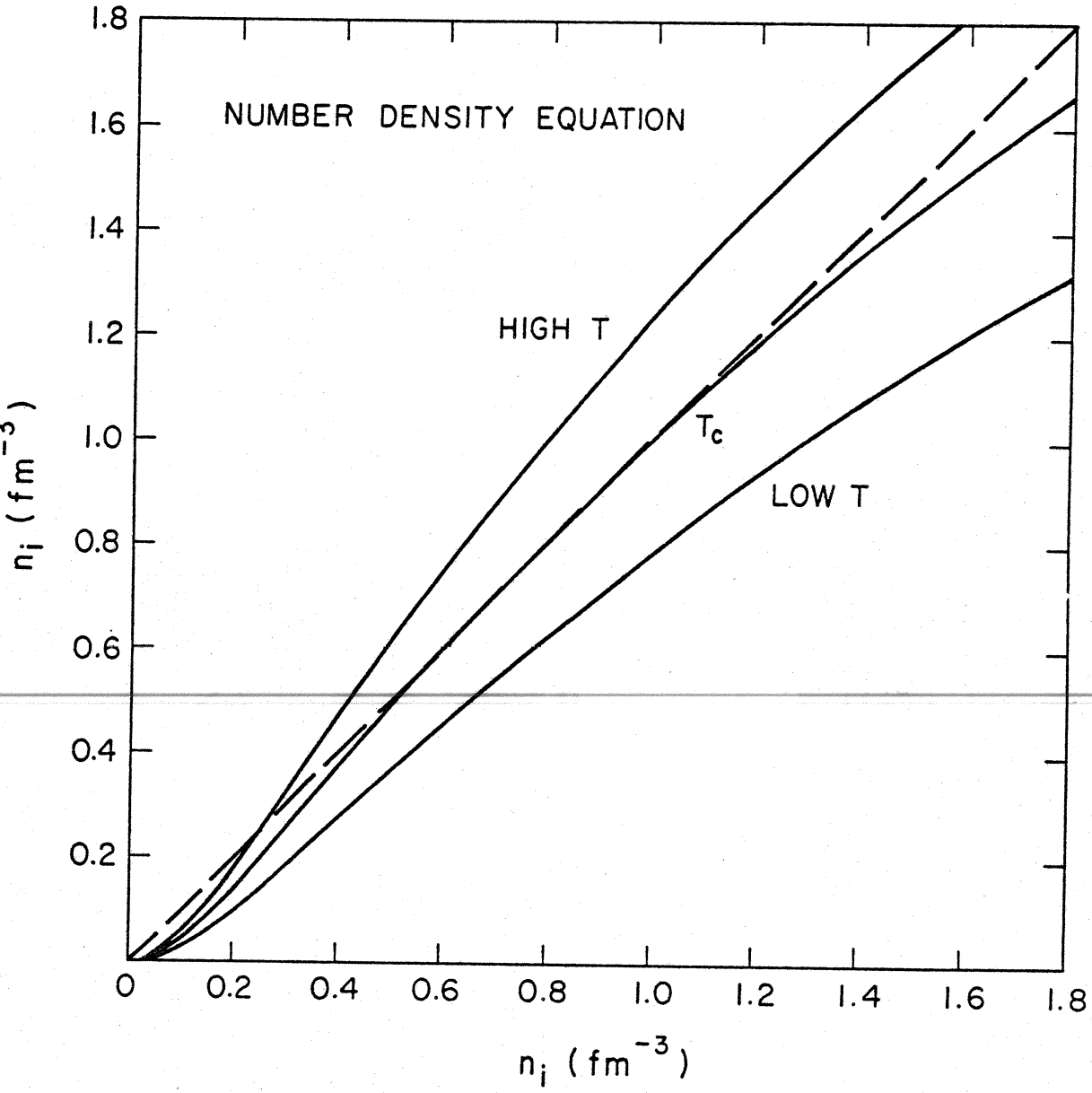
NUMBER DENSITY EQUATION
HIGH T
T_c
LOW T
n_i (fm^{-3})
n_i (fm^{-3})
0
0.2
0.4
0.6
0.8
1.0
1.2
1.4
1.6
1.8

FIG. 12

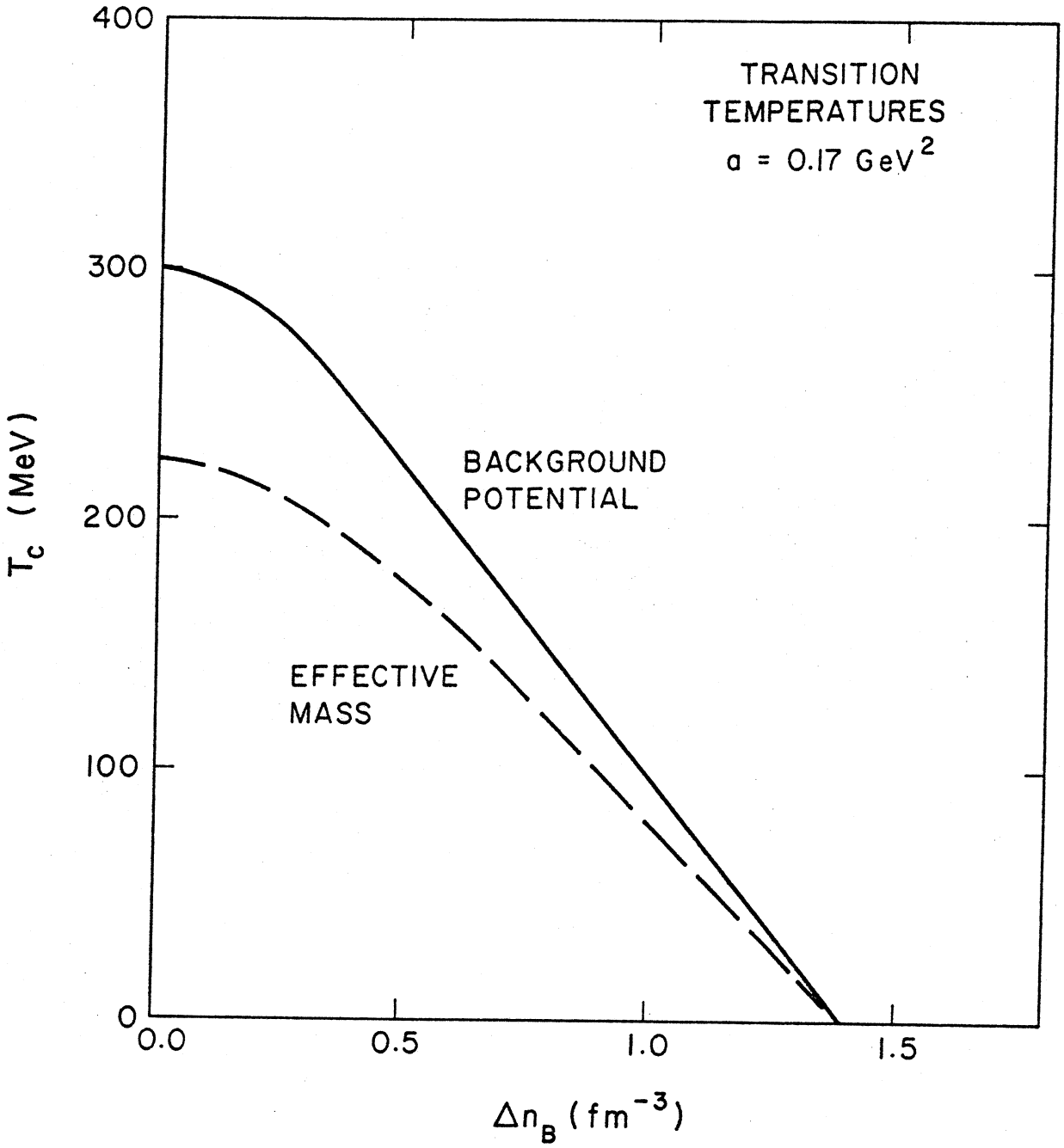
400
300
200
100
0
0.0
0.5
1.0
1.5
TRANSITION
TEMPERATURES
a = 0.17 GeV 2
BACKGROUND
POTENTIAL
EFFECTIVE
MASS
T_c (MeV)
Δn_B (fm^-3)

FIG. 13

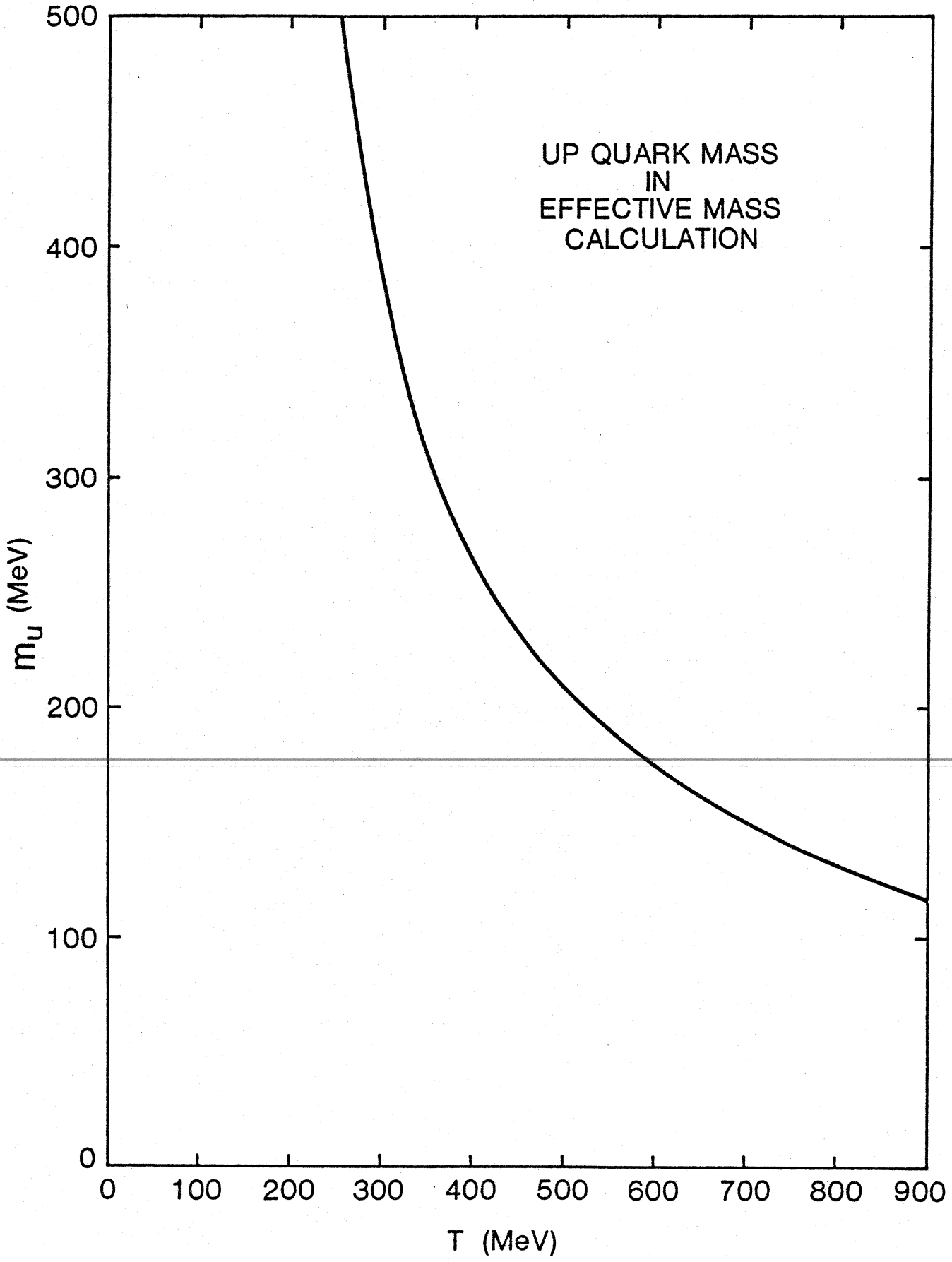
UP QUARK MASS
IN
EFFECTIVE MASS
CALCULATION
500
400
300
200
100
0
m_u (MeV)
0
100
200
300
400
500
600
700
800
900
T (MeV)

FIG. 14

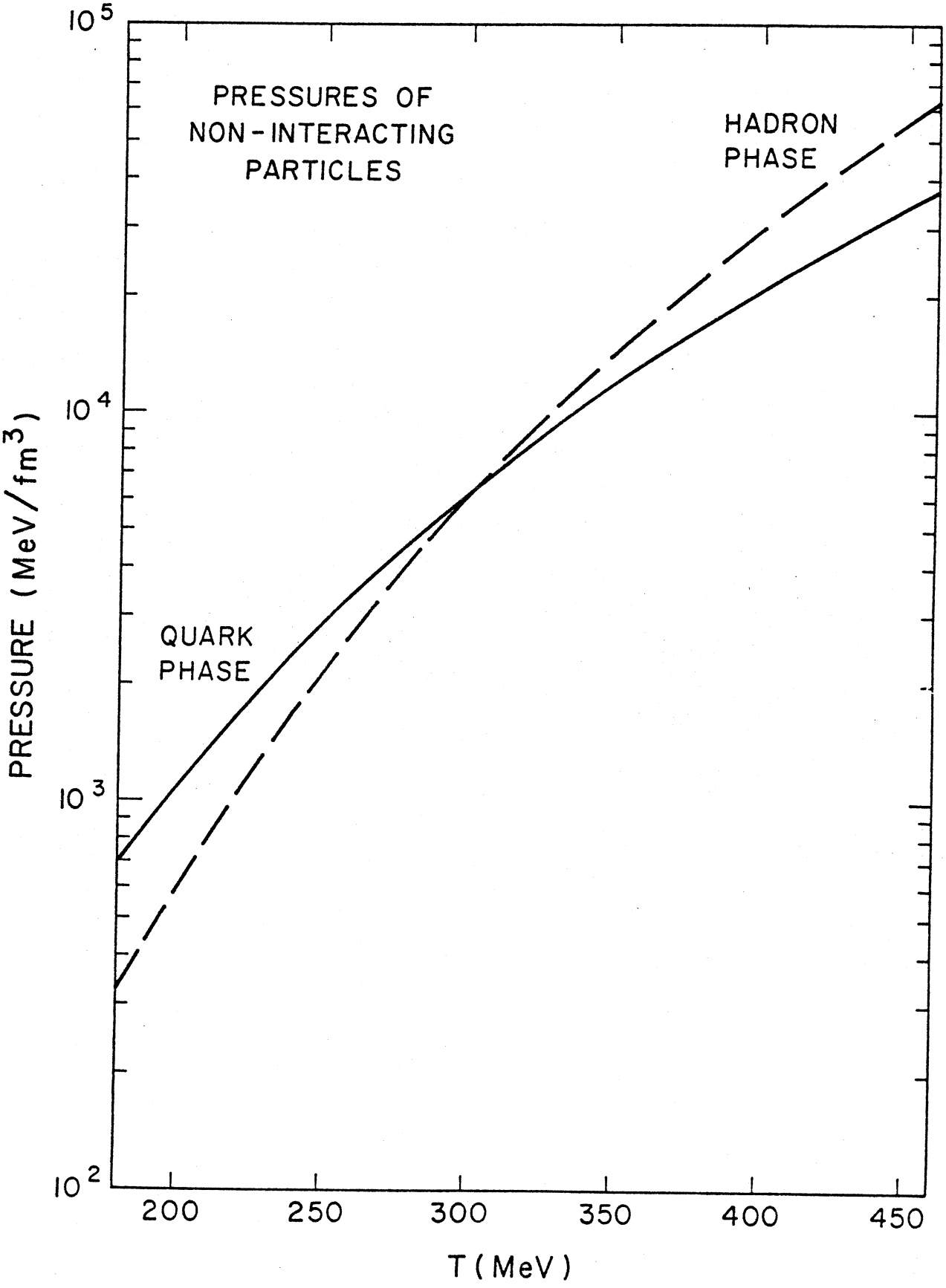
PRESSURES OF
NON-INTERACTING
PARTICLES
HADRON
PHASE
QUARK
PHASE
PRESSURE (MeV/fm^3)
10^5
10^4
10^3
10^2
200
250
300
350
400
450
T (MeV)

FIG. 15

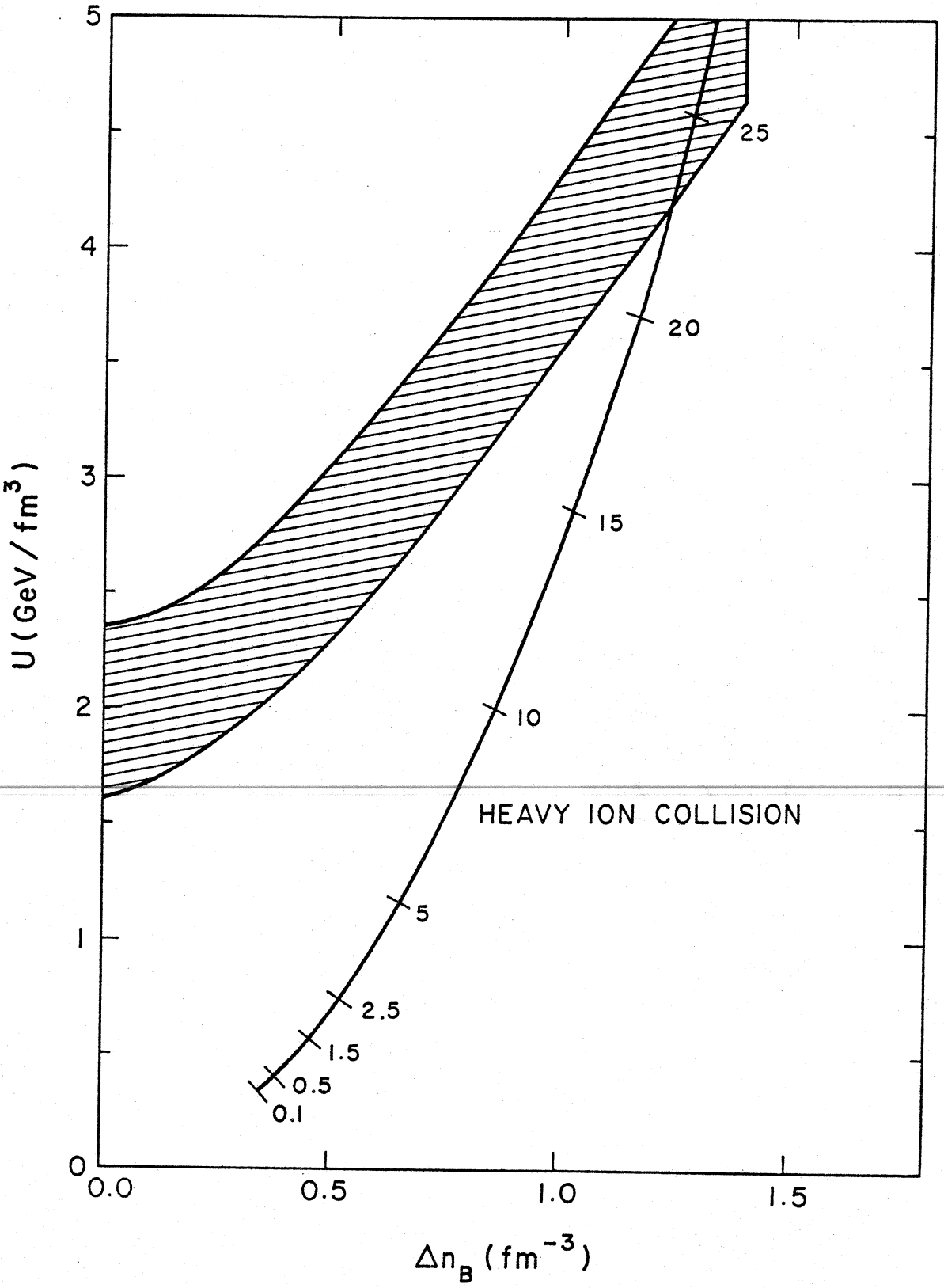
5
4
3
2
1
0
0.0
0.5
1.0
1.5
U (GeV / fm^3)
Δn_B (fm^{-3})
25
20
15
10
5
2.5
1.5
0.5
0.1
HEAVY ION COLLISION

FIG. 16

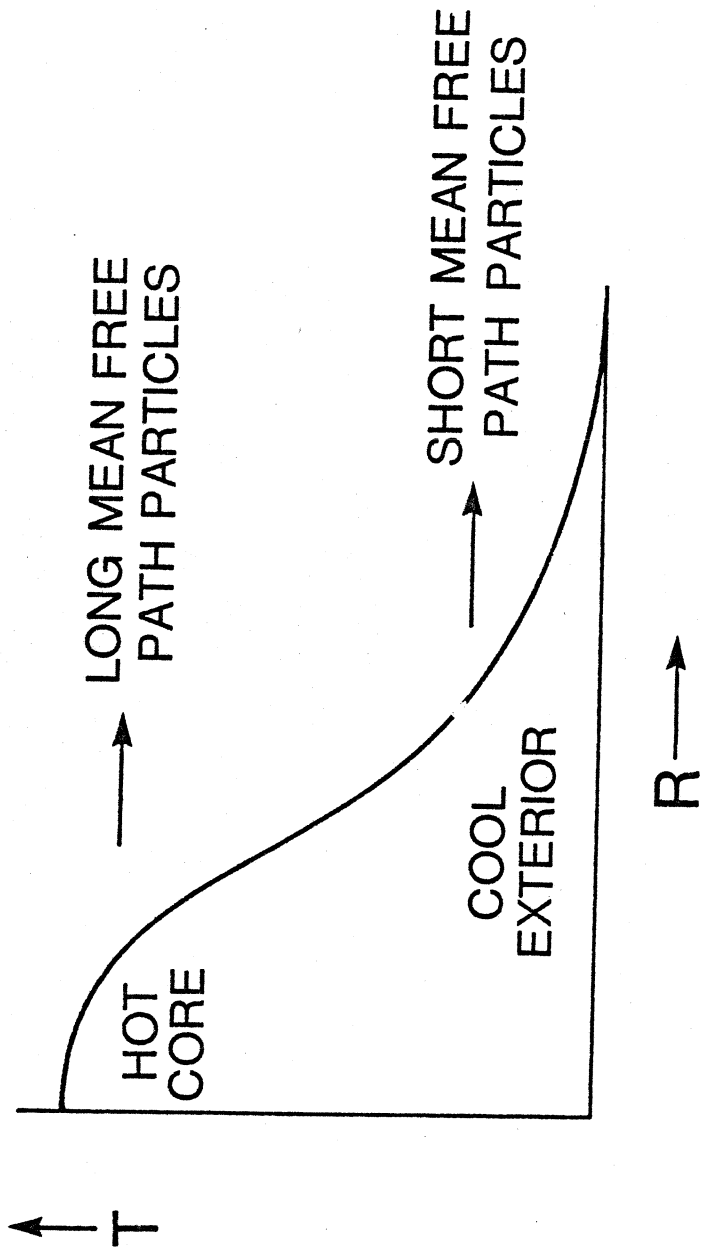
LONG MEAN FREE
PATH PARTICLES
SHORT MEAN FREE
PATH PARTICLES
HOT
CORE
COOL
EXTERIOR
T
R

FIG. 17

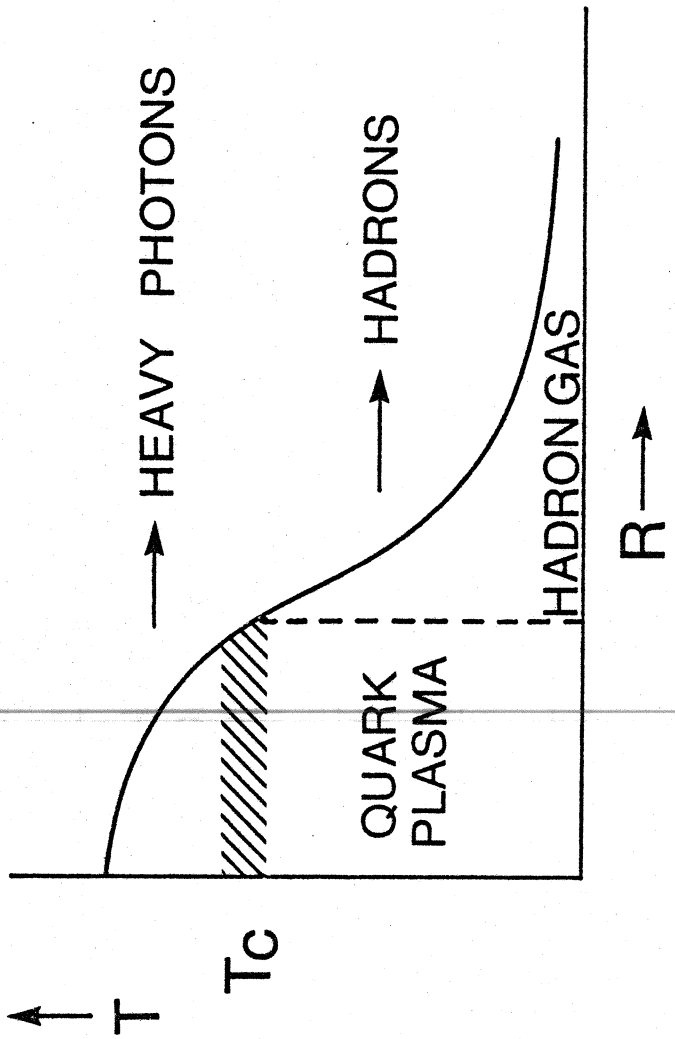

FIG. 18

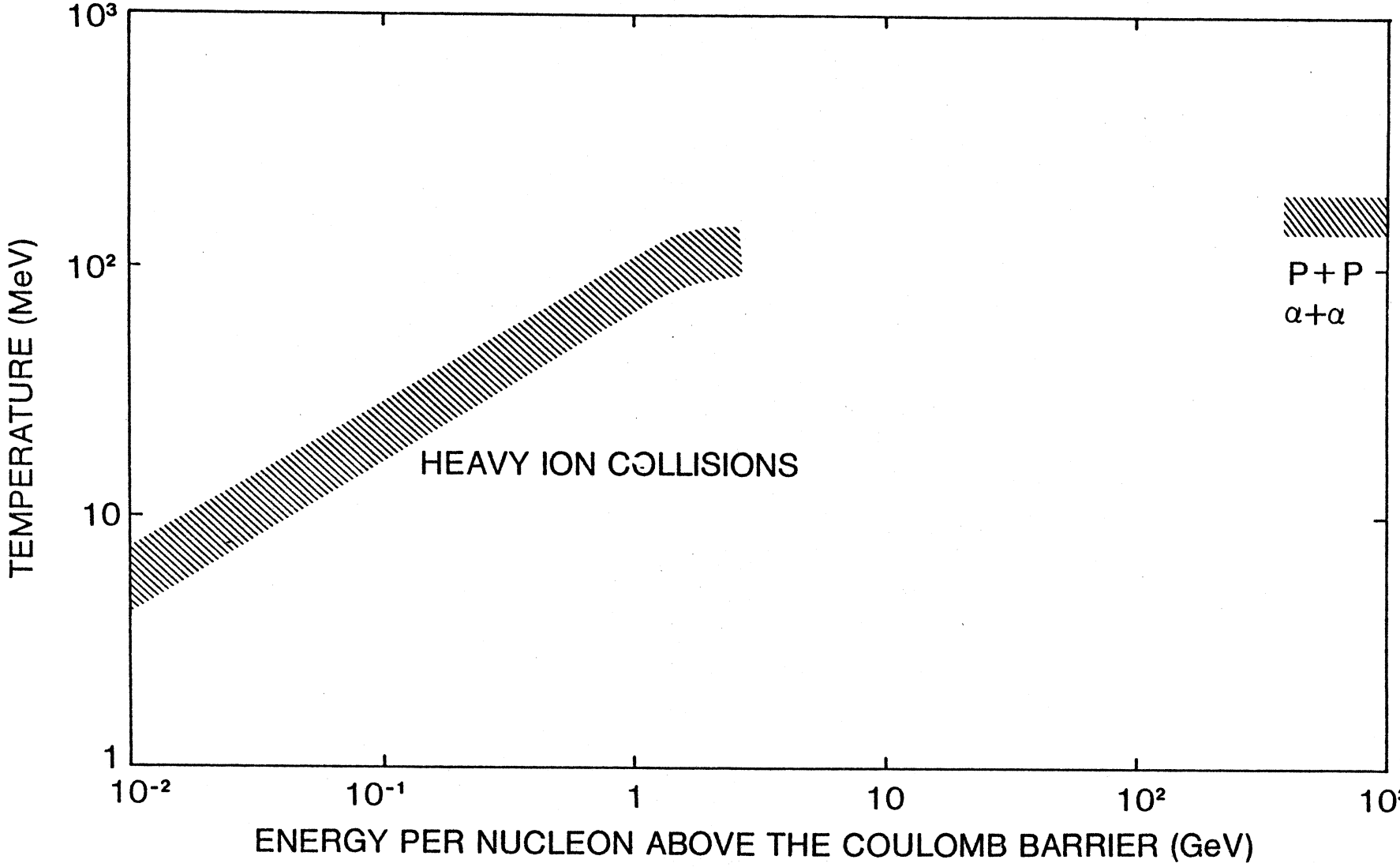
10^3
10^2
10
1
TEMPERATURE (MeV)
HEAVY ION COLLISIONS
P+P
α+α
10^{-2}
10^{-1}
1
10
10^2
10^3
ENERGY PER NUCLEON ABOVE THE COULOMB BARRIER (GeV)

Fig. 19

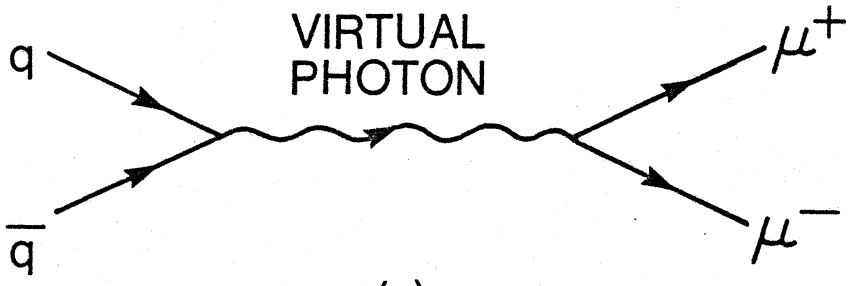

(a)

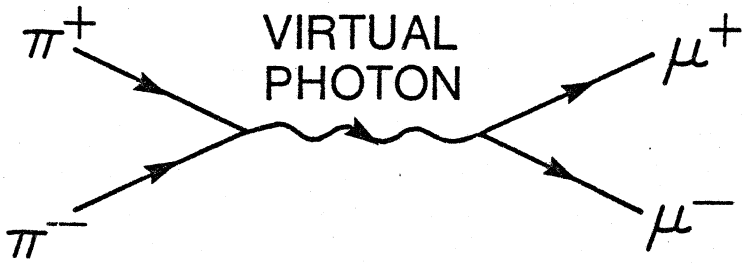

(b)

FIG. 20

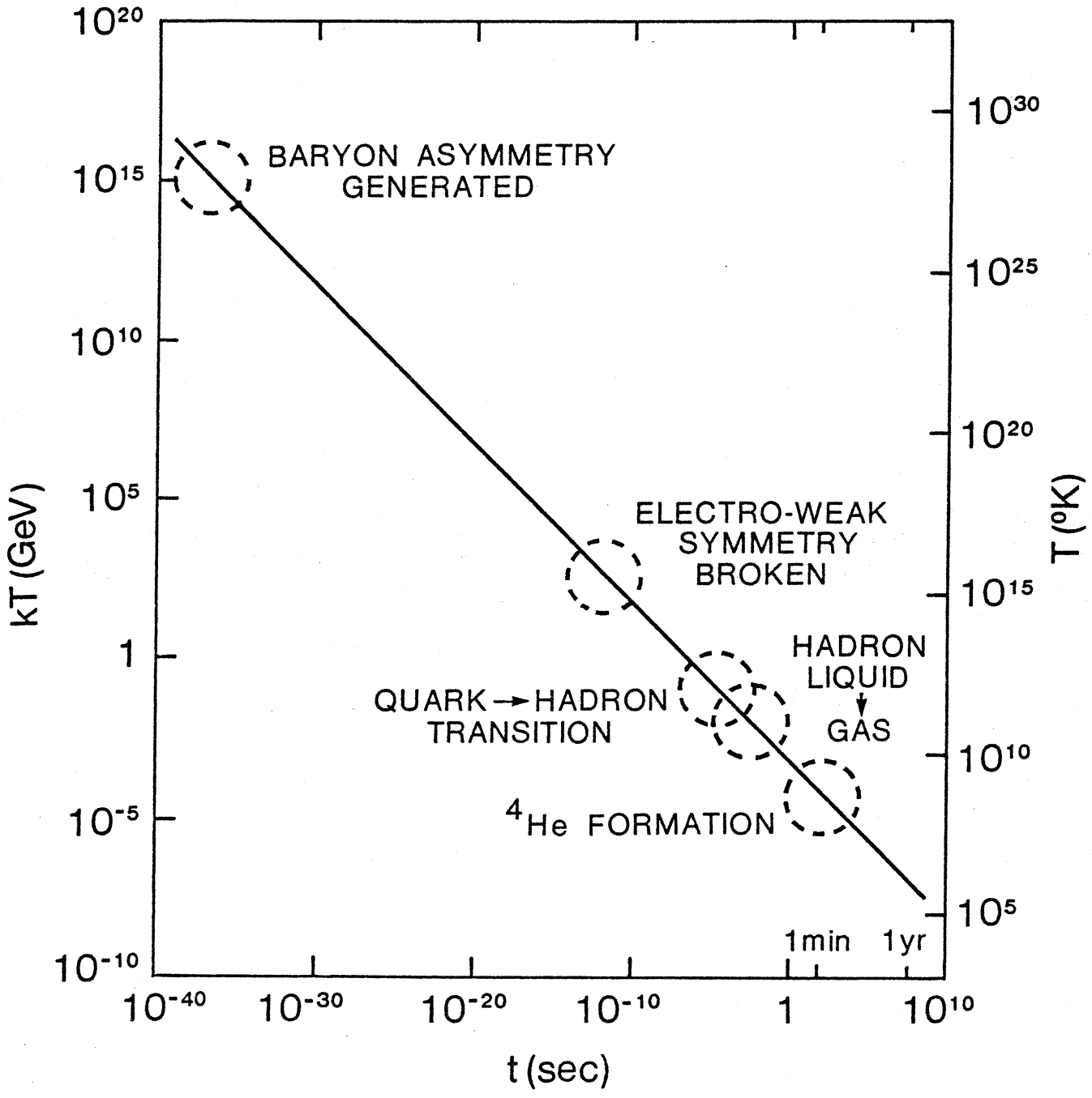
10^{20}
10^{15}
10^{10}
10^{5}
1
10^{-5}
10^{-10}
kT (GeV)
10^{30}
10^{25}
10^{20}
10^{15}
10^{10}
10^{5}
T (°K)
BARYON ASYMMETRY GENERATED
ELECTRO-WEAK SYMMETRY BROKEN
HADRON LIQUID
GAS
QUARK → HADRON TRANSITION
^{4}He FORMATION
1min
1yr
10^{-40}
10^{-30}
10^{-20}
10^{-10}
1
10^{10}
t (sec)

FIG. 21

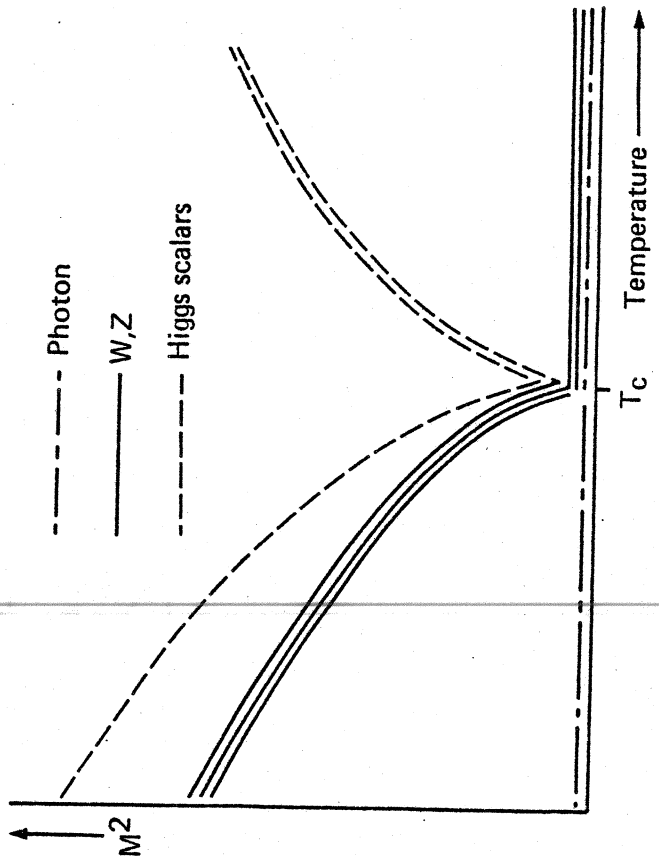

FIG. 22

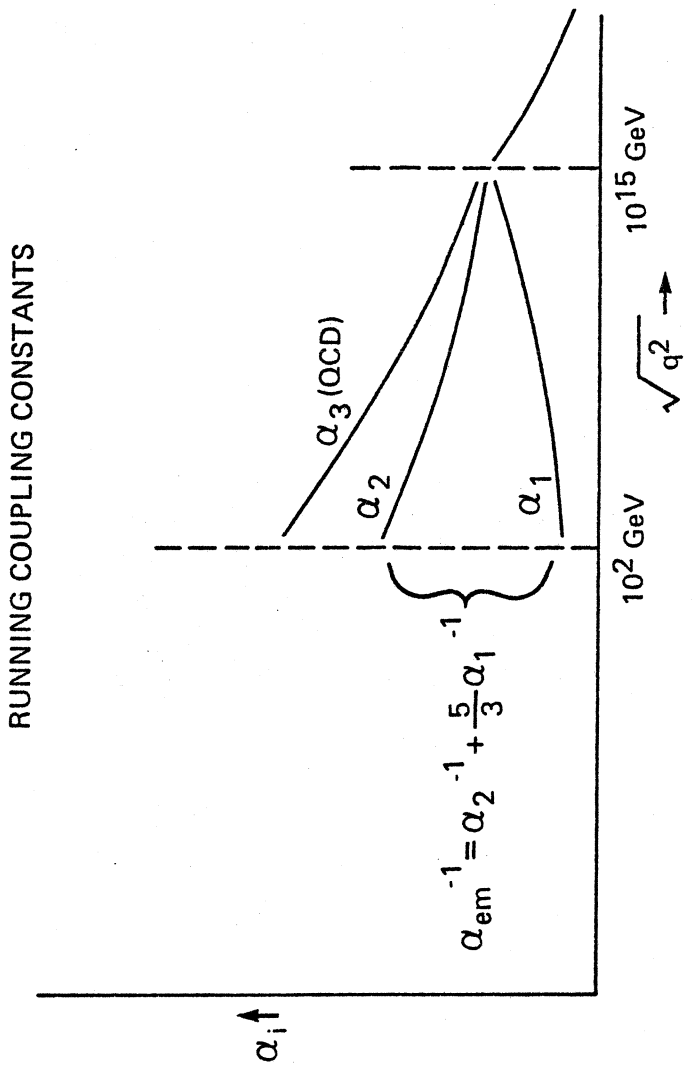
RUNNING COUPLING CONSTANTS
α_i
α_3 (QCD)
α_2
α_1
$\alpha_{em}^{-1} = \alpha_2^{-1} + \frac{5}{3}\alpha_1^{-1}$
10^2 GeV
10^{15} GeV
$\sqrt{q^2}$ →

FIG. 23

FIG. 24

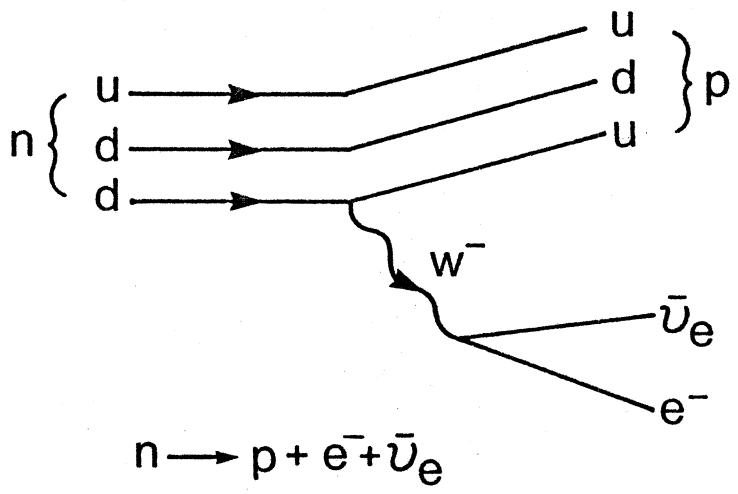

(a)

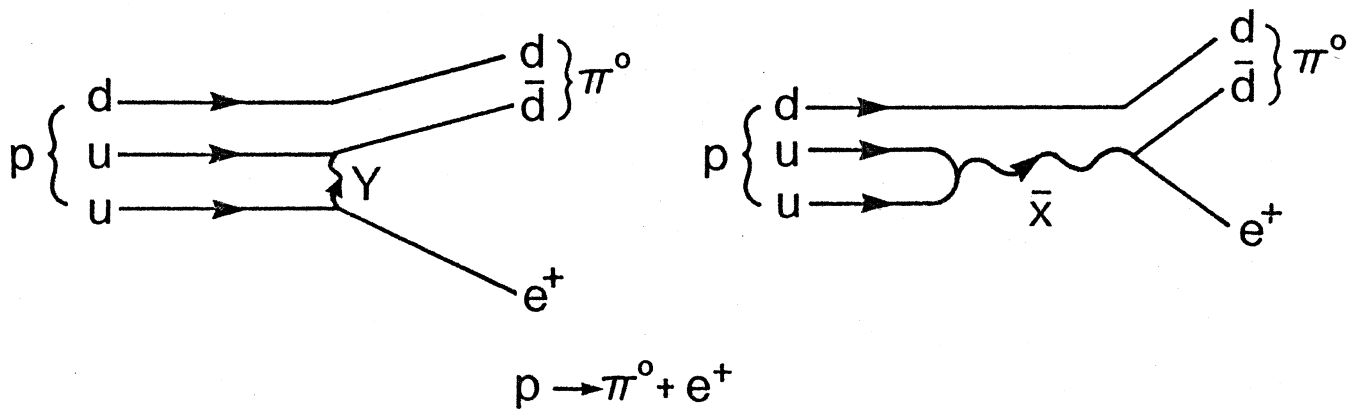

(b)

FIG. 25

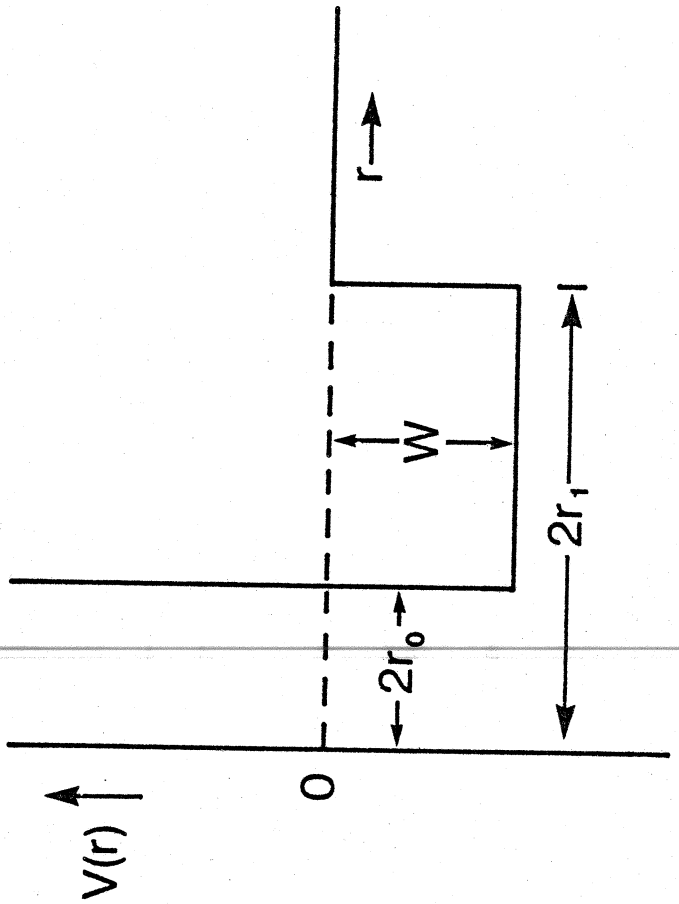

FIG. 26

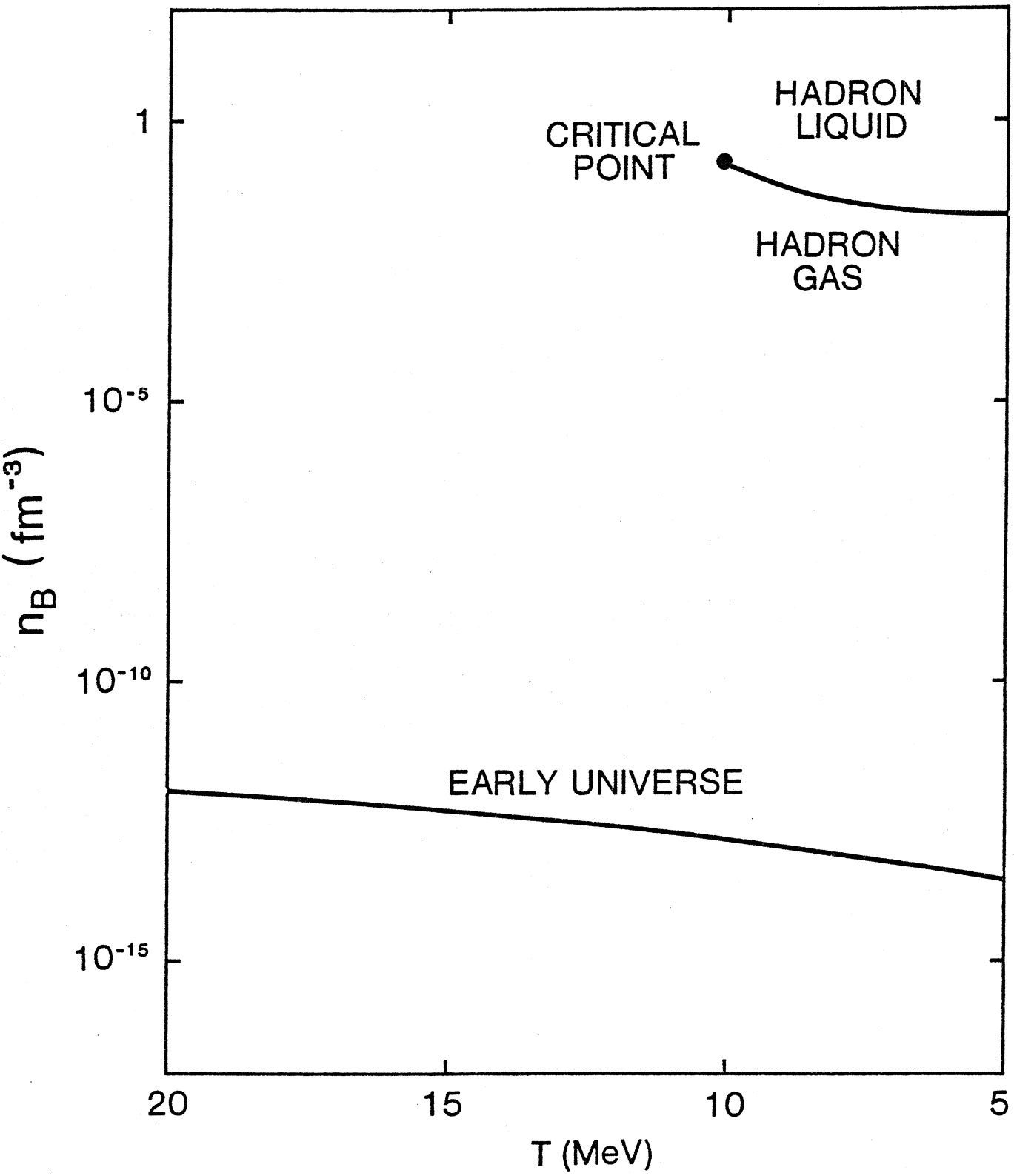
HADRON
LIQUID
CRITICAL
POINT
HADRON
GAS
EARLY UNIVERSE
1
10^{-5}
10^{-10}
10^{-15}
n_B (fm^{-3})
20
15
10
5
T (MeV)

FIG. 27

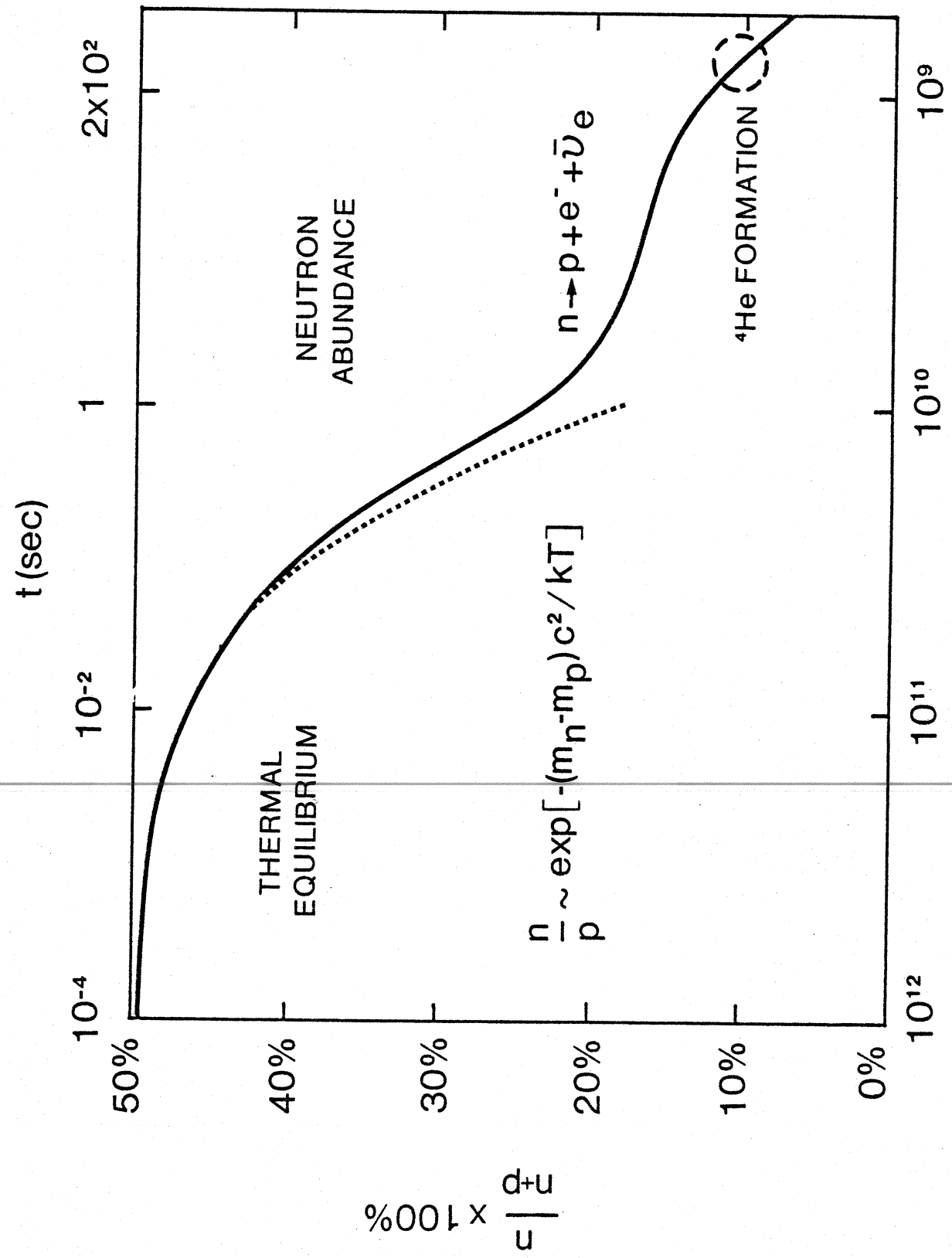
t (sec)
10-4
10-2
1
2x10²
T (°K)
10¹²
10¹¹
10¹⁰
10⁹
THERMAL EQUILIBRIUM
NEUTRON ABUNDANCE
n→p+e⁻+ν̄e
⁴He FORMATION
n/p ~ exp[-(mn-mp)c²/kT]
n/(n+p) x 100%
50%
40%
30%
20%
10%
0%

FIG. 28

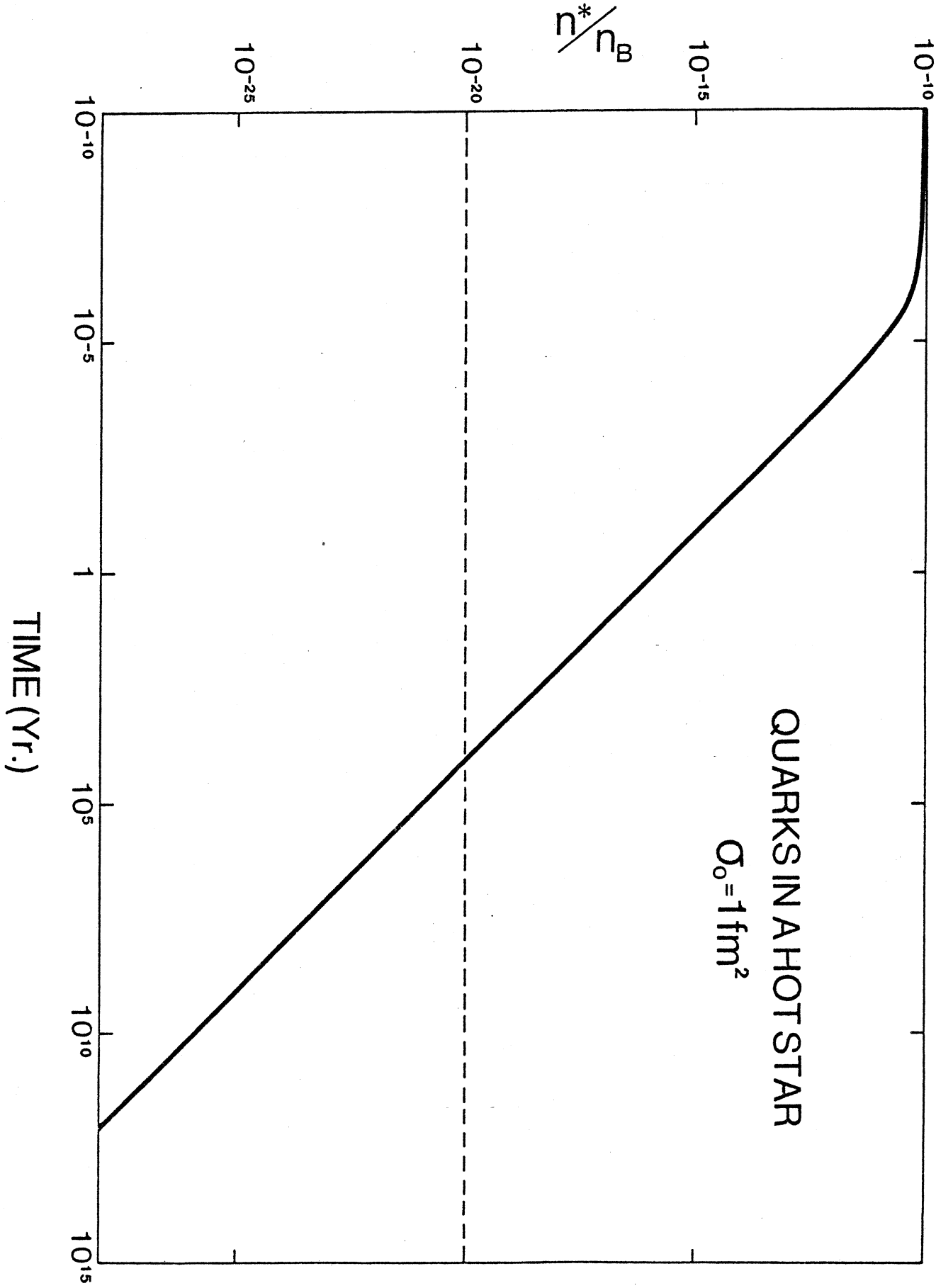
n^*/n_B
10^{-10}
10^{-15}
10^{-20}
10^{-25}
QUARKS IN A HOT STAR
$\sigma_0 = 1\,fm^2$
10^{-10}
10^{-5}
1
10^{5}
10^{10}
10^{15}
TIME (Yr.)

FIG. 29

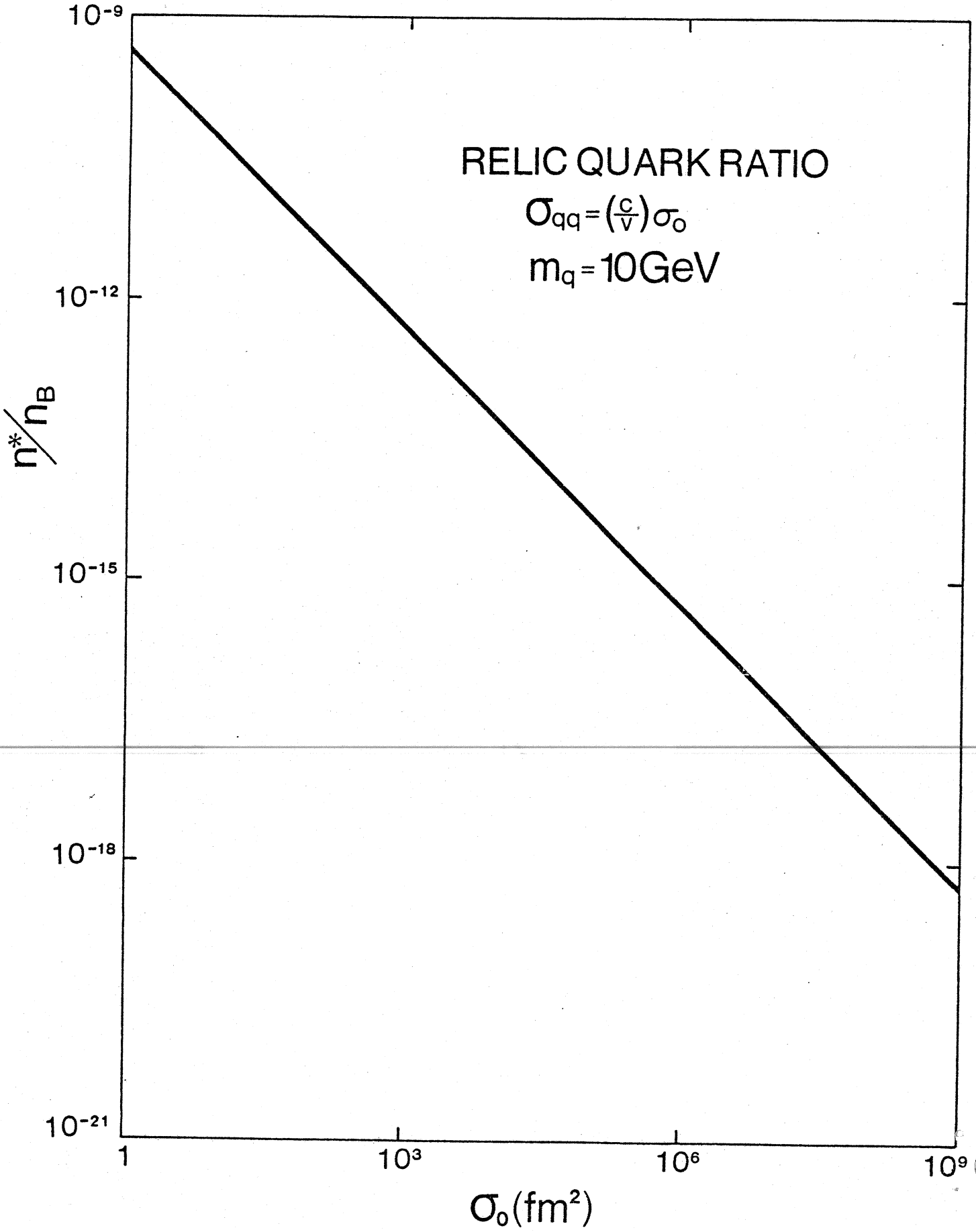
RELIC QUARK RATIO
$\sigma_{qq} = (\frac{c}{v})\sigma_o$
$m_q = 10GeV$
10^{-9}
10^{-12}
10^{-15}
10^{-18}
10^{-21}
n^*/n_B
1
10^3
10^6
10^9
$\sigma_o(fm^2)$

FIG. 30